UNIVERSIDADE FEDERAL DO CEARÁ
CENTRO DE CIÊNCIAS
DEPARTAMENTO DE BIOQUÍMICA E BIOLOGIA MOLECULAR
PROGRAMA DE PÓS-GRADUAÇÃO EM BIOQUÍMICA

VICTOR BRENO FAUSTINO BEZERRA

PAPEL FUNCIONAL DA FAMÍLIA DE ENZIMAS GLICOLATO OXIDASE (GOX) E CATALASE (CAT) EM FEIJÃO-CAUPI (*VIGNA UNGUICULATA* [L.] Walp.) NA RESPOSTA AO *COWPEA SEVERE MOSAIC VIRUS*

FORTALEZA
2025

VICTOR BRENO FAUSTINO BEZERRA

PAPEL FUNCIONAL DA FAMÍLIA DE ENZIMAS GLICOLATO OXIDASE (GOX) E CATALASE (CAT) EM FEIJÃO-CAUPI (*VIGNA UNGUICULATA* [L.] Walp.) NA RESPOSTA AO *COWPEA SEVERE MOSAIC VIRUS*

Dissertação apresentada ao Programa de Pós-Graduação em Bioquímica da Universidade Federal do Ceará, como requisito parcial à obtenção do título de Mestre em Bioquímica. Área de concentração: Bioquímica Vegetal.

Orientador: Prof. Dr. Murilo Siqueira Alves

FORTALEZA

2025

VICTOR BRENO FAUSTINO BEZERRA

PAPEL FUNCIONAL DA FAMÍLIA DE ENZIMAS GLICOLATO OXIDASE (GOX) E CATALASE (CAT) EM FEIJÃO-CAUPI (*VIGNA UNGUICULATA* [L.] Walp.) NA RESPOSTA AO *COWPEA SEVERE MOSAIC VIRUS*

Dissertação apresentada ao Programa de Pós-Graduação em Bioquímica da Universidade Federal do Ceará, como requisito parcial à obtenção do título de Mestre em Bioquímica. Área de concentração: Bioquímica Vegetal.

Aprovada em: 28/02/2025.

BANCA EXAMINADORA

_____

Prof. Dr. Murilo Siqueira Alves (Orientador)
Universidade Federal do Ceará (UFC)

_____

Prof. Dr. Humberto Henrique de Carvalho
Universidade Federal do Ceará (UFC)

_____

Dra. Stelamaris de Oliveira Paula Marinho
Universidade Federal do Ceará (UFC)

AGRADECIMENTOS

Ao Prof. Dr. Murilo Siqueira Alves pela excelente orientação, e por sempre nos motivar como ser humano e pesquisadores. E por ser aquele que nunca deixou de acreditar em todos nós sempre.

Aos professores participantes da banca examinadora Prof. Dr. Humberto Henrique de Carvalho e Dra. Stelamaris de Oliveira Paula Marinho pelo tempo, pelas valiosas colaborações e sugestões, e pela compreensão durante todo o processo do desenvolvimento da presente dissertação.

Aos colegas da turma de mestrado e do Departamento de Bioquímica e Biologia Molecular (DBBM) que foram importantes para o meu crescimento como pesquisador e pessoa. E aos meus amigos, Leonardo Elias Araújo dos Santos e Mateus Viggiano de Almeida Dondi, que mais que amigos, já são como irmãos para mim.

A todos os integrantes do Laboratório de Sinalização Celular de Plantas (LabSin), Jochuan Israel Bezerra do Nacimento, Otávio Hugo Aguiar Gomes, Érica Monik Silva Roque e Felipe de Castro Texeira. E especialmente os estudantes de graduação João Victor Dourado Alves Britos, Gabriela Oliveira Matos e Lorenna Maria Neves Freitas, que com toda a certeza se não estivessem presentes esse trabalho seria impossível, os agradeço imensamente.

Ao Laboratório de Fisiologia Vegetal (LabFive) pela bela parceria com nosso laboratório, e sempre me receber de forma solicita e acolhedora, e se fosse de outra forma o presente trabalho teria sido impossível de ser finalizado. Agradeço a todos os seus integrantes, principalmente a estudante de doutorado Isabelle Mary Costa Pereira, que sempre me iluminou com ideias e esperança em momentos difíceis.

A minha família em especial aos meus pais, Renata Faustino dos Santos Bezerra, José Luciano Bezerra Júnior, e minha avó, Maria Valdete Faustino da Silva, por serem os agentes que tornaram possível o meu desenvolvimento.

E especialmente a minha noiva Taís Bentemüller Pinto, que sempre me incentivou a me manter seguro ao meu sonho como pesquisador e a ser uma pessoa melhor sempre, e é indispensável para o que o sou hoje.

O presente trabalho foi realizado com o apoio da Coordenação de Aperfeiçoamento de Pessoal de Nível Superior – Brasil (CAPES) – Código de financiamento 001

RESUMO

Com o aumento do déficit alimentar e carência nutricional, a escolha por culturas alternativas e de características relevantes se fazem importantes. Com isso, *Vigna unguiculata* L. se faz como uma cultura de grande interesse. Entretanto, o feijão-caupi ainda é susceptível a alguns patógenos, como no caso do *CowPea Severe Mosaic Virus* (CPSMV). Em condições adversas, como infecção por patógenos, um dos mecanismos iniciais para a resposta ao estresse envolve a produção de espécies reativas de oxigênio. Uma dessa moléculas é o peróxido de hidrogênio, que tem sua maior taxa de produção relacionada a Glicolato Oxidase (GOX), uma enzima do processo de fotorrespiração. Mas, como toda espécie reativa, sua produção e consumo devem ser balanceados finamente, assim a enzima Catalase (CAT) é responsável por esse controle durante um fenômeno de estresse. Logo, o presente trabalho teve como objetivo analisar a expressão das cópias génicas da enzima GOX e CAT, a nível de transcrito e de atividade, em resposta ao CPSMV. Para tal, os exemplares vegetais foram inoculados com o CPSMV em 3 pontos ao longo do tempo (16 horas, 48 horas e 144 horas). Análises de atividade enzimática da catalase demonstraram diferenças entre os cultivares apenas nas horas iniciais (16h), nas condições controle de Pitiúba inoculada e *Mock*. Além disso, análises com coloração por DAB (3,3'-Diaminobenzidina), MDA (Malonaldeído) e conteúdo de peróxido foi utilizado para constatar o grau de estresse oxidativo, novamente com diferenças apenas entre Pitiúba *Mock* e inoculado nas coletas de 16 e 48h. Dados de expressão demonstraram diferenças principalmente no gene *VuGOX1* no cultivar Macaíbo sendo induzida sua expressão durante a infecção em comparação ao *Mock*. Enquanto *VuGOX2* foi o gene com a maior abundância a nível de transcrito, apresentando diferenças entre os cultivares nos tempos de 16 e 144h, com a expressão reduzida em Pitiúba inoculado em comparação com o *Mock* 144h. Análises de bioinformática, como elementos cis, filogenia e previsão de localização subcelular, demonstrou características relacionadas à resposta a vários estresses. Assim, nossos dados sugerem que o complexo GOX-CAT durante a resposta ao patógeno, modulando sua resposta local e sistemicamente. Assim, é esperado que os resultados encontrados ajudem programas de melhoramento e o entendimento sobre o fenômeno de resistência.

Palavras-chave: Fotorrespiração; *Comovirus*; ácido salicílico; resistência; GOX-CAT *switch*

ABSTRACT

With the increase in food shortages and nutritional deficiencies, the choice of alternative crops with relevant characteristics is important. *Vigna unguiculata* L. is therefore a crop of great interest. However, cowpeas are still susceptible to some pathogens, such as the *CowPea Severe Mosaic Virus* (CPSMV). Under adverse conditions, such as infection by pathogens, one of the initial mechanisms for the stress response involves the production of reactive oxygen species. One of these molecules is hydrogen peroxide, which has its highest production rate related to Glycolate Oxidase (GOX), an enzyme in the photorespiration process, but like all reactive species, its production and consumption must be finely balanced, so there is the peroxisomal enzyme Catalase (CAT), responsible for this control during a stress phenomenon. The aim of this study was therefore to analyse the expression of GOX and CAT gene copies, at transcript and activity level, in response to CPSMV. To this end, the plant specimens were inoculated with CPSMV at three time points (16 hours, 48 hours and 144 hours). Analyses of catalase enzyme activity showed differences between the cultivars only in the initial hours (16h), in the control conditions of inoculated Pitiúba and Mock, possibly related to the initial response to the pathogen. In addition, analyses using DAB (3,3'-Diaminobenzidine) staining, MDA (Malonaldehyde) and peroxide content were used to determine the degree of oxidative stress, again with differences only between Pitiúba Mock and inoculated at 16 and 48 hours. In addition, the expression data showed differences mainly in the VuGOX1 gene in the Macaíbo cultivar, whose expression was induced during infection compared to the Mock. While VuGOX2 was the gene with the highest abundance at transcript level, showing differences between the cultivars at times of 16 and 144h, with reduced expression in inoculated Pitiúba compared to Mock 144h. Bioinformatics analysis, such as cis-elements, phylogeny and sub-cellular localisation prediction, demonstrated characteristics related to the response to various stresses. Thus, our data suggest that the GOX-CAT switch complex acts during the response to the pathogen, modulating its response locally and systemically. Thus, it is hoped that the results found will help breeding programmes and understanding of the resistance phenomenon.

Keywords: photorespiration; *Comovirus;* qPCR; hydrogen peroxide; resistence*;* genetic expression.

SUMÁRIO

1 FUNDAMENTAÇÃO TEÓRICA 09
1.1 ***Vigna unguiculata*** 09
1.2 ***Cowpea Severe Mosaic Virus*** **(CPSMV)** 10
1.3 Glicolato oxidase e Catalase 13
REFERÊNCIAS 18
2 OBJETIVOS 17
2.1 Objetivo geral 17
2.2 Objetivos específicos 17
3 MANUSCRITO 25

REFERÊNCIAS 50
ANEXO DE PRODUTIVIDADE..... 76

1.FUNDAMENTAÇÃO TEÓRICA

1.1 *Vigna unguiculata*

O feijão-caupi (*Vigna unguiculata* [L.] Walp.), denominado popularmente feijão-de-corda, feijão-fradinho ou feijão massacar, é um membro da família Fabaceae, da ordem Fabales, classe Magnoliopsida (Carvalho *et al.*, 2017). Tal espécie é amplamentecultivada em regiões de clima subtropical e tropical, como no continente africano, parte da Ásia, e na América Latina, onde no Brasil, especificamente, tem seu cultivo focado nas regiões Norte, Nordeste e Centro-Oeste (Duraipandian *et al*., 2022). A prevalência do cultivo do feijão-caupi nessas regiões deve-se àsua grande tolerânciaao déficit hídrico, tendo em vista que são regiões, em sua maioria, de baixa pluviosidade (Martins *et al.*, 2003; Hall *et al*., 2003; Bastos, 2017). Ademais, a leguminosa possui um alto teor nutricional agregado, contando com grande concentração de proteínas e aminoácidos essenciais em seus grãos secos e verdes, vagens e folhas, além de alto conteúdo de fibra alimentar e macro e micronutrientes (Silveira *et al*., 2001; Gonçalves *et al*., 2016; Carvalho *et al.*, 2017). A espécie também possui um papel agroecológico relevante, devido à sua relação simbiótica com bactérias fixadoras de nitrogênio, enriquecendo o solo para o cultivo de outras culturas e do próprio feijão-caupi (Silveira *et al*., 2001; Gonçalves *et al*., 2016).

Devido às características de alto valor nutricional e tolerância à seca, o feijão-caupi é um organismo candidato para estudos de melhoramento genético e engenharia genética de plantas, visando a produção de novos cultivares (Pereira *et al.*, 2014). Nos últimos anos, cultivares de *V. unguiculata* vêm sendo amplamente utilizados para o estudo de tolerância a estresses ambientais, principalmente ao déficit hídrico (Carvalho *et al.*, 2019; Gomes *et al.*, 2020; Jayawardhane *et al.*, 2022). Entretanto, além dos estresses abióticos, o feijão-caupi enfrenta grandes desafios devido àação de patógenos e pragas, capazes de afetar o indivíduo vegetal em todas as fases do desenvolvimento (Allen, 1983). Em relação às fitopatologias causadas por vírus, as perdas de produtividade podem variar de 10% até casos de 100%, dependendo das relações entre hospedeiro e vetor (Raheja; Leleji, 1975; Shoyinka, 1997; Kareem; Taiwo, 2007).

Apesar de não se tratar de uma espécie modelo tradicional, nos últimos anos a utilização do feijão-caupi como objeto de estudo vem sendo cada vez mais empregada, com estudos nas áreas multi-ômicas, para melhor entender seus mecanismos genéticos,

fisiológicos e moleculares, visando a utilização de técnicas de melhoramento vegetal (Ferreira-Neto *et al.*, 2021; Omomowo, 2021).

1.2 *Cowpea Severe Mosaic Virus* (CPSMV)

Como comentado anteriormente, diversos estímulos podem acabar impactando negativamente o desenvolvimento e produtividade de espécies cultivadas, incluindo tanto estresses de origem abióticas como bióticas (Nawaz *et al.*, 2023). Os impactos de estresse abiótico são amplamente descritos, como no caso de seca/escassez hídrica, alagamento, salinidade alta, toxicidade ou escassez por nutrientes, temperaturas extremas ou estresse osmótico (Zhang *et al.*, 2023). Entre os tipos de estresse biótico um dos principais são os vírus, já que com as mudanças das dinâmicas das temperaturas no mundo nas últimas décadas, houve um aumento na distribuição de vários vetores de vírus, o que fez com que os patógenos entrassem em contato com novos potenciais vetores (Trebicki, 2020). Isso pode levar a um impacto em diversas espécies cultivadas, e trazendo problemas de abastecimento de comida ao redor do mundo.

Os vírus são um grupo taxonômico capaz de infectar um grande número de hospedeiros, que vão desde bactérias, animais, até plantas. Entre os hospedeiros, os indivíduos vegetais são aqueles que mais apresentaram um aumento no número de patógenos infectando novas espécies (Anderson *et al*., 2004; Stukenbrock; McDonald, 2008). Como já comentado, os vírus trazem consigo perda de qualidade e produtividade, além de agravar o problema de insegurança alimentar no mundo, onde as perdas em espécies cultivadas foram responsáveis por cerca de U$20 bilhões de dólares, e com as perdas estimadas totais chegando a U$60 bilhões (Zhao *et al*., 2017).

Entre os diversos gêneros de vírus existentes, o *Comovirus* que faz parte da subfamília Comovirinae, da família Secoroviridae, compreende vírus de genomas bipartidos e encapsulados em proteínas (Fuchs et al., 2022; ICTV, 2025). O RNA-1 e RNA-2 são ambos RNA de fita simples (ssRNA) com uma orientação positiva (+), ambos apresentado uma calda poli-A, e porções N- e C-terminal, com seus vírions compostos por 60 copias de dois tipos de polipeptídeos, cada um com três diferentes estruturas (Goldbach; Wellink, 1996; Carette et al., 2002; Pouwels et al., 2002; Thompson et al., 2017). Com dois tipos de polipeptídeos se unindo no capsídeo viral, um grande e outro pequeno (Figura A), que são traduzidas pelo RNA-2, sendo vital para o movimento viral entre células (Thompson *et al*., 2017; Texeira *et al*., 2021). Além disso, a molécula de

RNA-2 viral é responsável por codificar duas poliproteínas que se sobrepõem, que por clivagem diferencial, resultam em três domínios, que irão codificar para a proteína grande do capsídeo (CP-L; *capside large-protein*; 40-45 kDa), a proteína pequena do capsídeo (CP-S; *capside small-protein*; 21-27 kDa), e a proteína de movimento (MP*; movement protein*) (Carette *et al*., 2002; Sanfaçon *et al*. 2009; Thompson *et al*., 2017; Texeira *et al*., 2021; ICTV, 2025).

Figura A. Representação molecular da partícula do vírus do mosaico do feijão-caupi (CPMV), com a parte superior representando A: proteína pequena do capsídeo, B: domínio C-terminal da proteína grande do capsídeo e C: domínio N-terminal da proteína grande do capsídeo. Parte inferior com três partículas de *Comovirus* com a partícula B contendo uma molécula de RNA-1, a partícula M contendo o RNA-2, e a partícula T vazia.

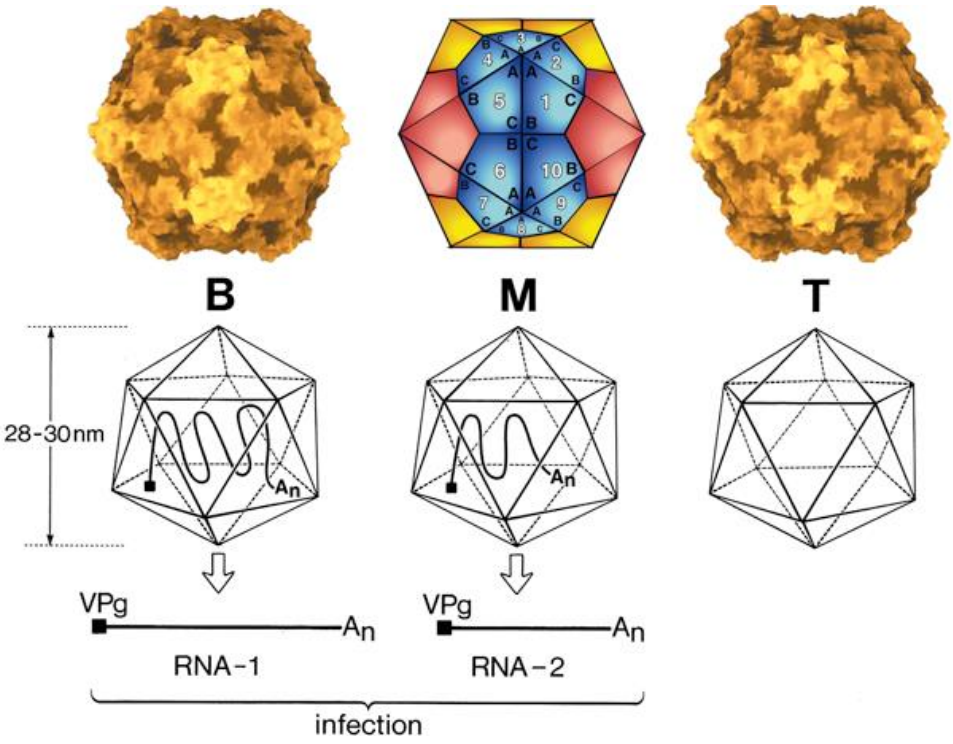

Fonte: ICTV (https://ictv.global/report_9th/RNApos/Picornavirales/Secoviridae)

Enquanto o RNA-1 é responsável por codificar uma única poliproteína que será processada em cinco domínios através de processos alternativos de clivagem (Figura B), relacionados ao processo de replicação viral (Texeira et al., 2021). Na sua porção N-terminal, há o cofator proteico (Co-Pro; 32 kDa), que é gerado após a primeira clivagem,

importante para o processamento da poliproteína gerada nos processos de clivagem seguintes (Thompson et al., 2017). Após isso, o restante da proteína terá processos de clivagens alternativas formando os quatro domínios restantes (Figura B), sendo esses a helicase de ligação a NTP (NTB; *NTB-biding helicase*; 58 kDa), proteína viral de ligação ao genoma (VPg; *viral protein genome-linked*), a proteinase (Pro; 24 kDa), e a RNA polimerase dependente de RNA (Pol; RNA-dependent RNA polymerase; 87 kDa) (Peters et al., 1994; Carette et al., 2002; Pouwels et al., 2002; Thompson et al., 2017; Oliveira et al., 2020; Texeira et al., 2021).

O gênero possui 19 espécies distintas, onde são principalmente caracterizados pelo sintoma do mosaico característico, com a maioria dos seus vetores sendo compostos principalmente por insetos da família Chrysomelidae, com um gama de hospedeiros sendo bem restrito para indivíduos vegetais da família Fabaceae (Cassell, 2011; Thompson et al., 2017; ICTV, 2025). E entre as espécies dos vírus o Vírus do Mosaico Severo do Caupi (CPSMV; *Cowpea Severe Mosaic Virus*) foi inicialmente confundido com uma cepa do vírus do mosaico do caupi (CPMV; *Cowpea Mosaic Virus*), entretanto apresentando sintomas de formas mais severas, e posteriormente diferenciado por teste de serologia realizadas em regiões da América Central e do Sul (Fulton, 1979; Chen; Bruening; 1992).

Figura B. Organização genômica e os processos de clivagem da poliproteína do vírus do mosaico do feijão-caupi (CPMV). MP: proteína de movimento; CP-L e CP-S: proteína grande e pequena do capsídeo, respectivamente; Co-Pro: cofactor da proteinase; NTB: proteína de ligação ao NTP; Pro: proteinase; Pol: RNA polimerase dependente de RNA. Círculo preto representando a extremidade 5'- do RNA, enquanto A(n) na extremidade 3'- representa a cauda poli-A.

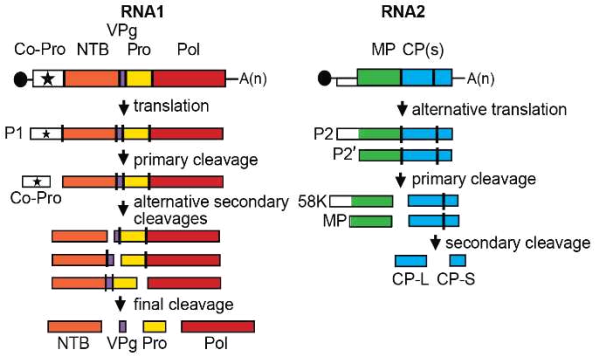

Fonte: ICTV (https://ictv.global/report/chapter/secoviridae/secoviridae/comovirus)

Os isolados de CPSMV no Brasil apresenta grande similaridade de sequência de nucleotídeos, variando entre 92-100%, demonstrando uma grande estabilidade genética, com diferenças do isolado dos EUA, mais comumente utilizado como referência em pesquisas (Lima et al., 2012; Texeira et al., 2021). Como previamente comentado, o CPSMV, como a maioria dos vírus do gênero *Comovirus* tem como hospedeiro espécies da família Fabaceae, sendo as culturas de maior interesse a soja, devido a sua importância econômica (*Glycine max* L.) e o feijão-caupi (Kitajima, 2020). Entre os sintomas causados pelo vírus os comuns são manchas cloróticas, manchas irregulares, bolhosidades, folhas retorcidas e/ou reduzidas, e o padrão clássico de mosaico, com a severidade dos sintomas variando de acordo com a espécies e cultivar infectado, onde as perdas de produtividade podem chegar a 85% (Booker et al., 2005; Booker et al., 2007; Souza et al., 2017).

1.3 Glicolato Oxidase e Catalase

As plantas, devido a sua natureza séssil, durante o processo evolutivo acabaram por desenvolver diversos mecanismos a fim de contornarem diferentes cenários de estresses provenientes do ambiente e de outros organismos. Comumente em situações de estresse, as plantas têm como resposta o fechamento estomático seguido como consequência o processo de fotorrespiração ocorre, visando uma forma de evitar a perda de água e a manutenção do metabolismo por meio de uma rota energética diferente da fotossíntese (Sharkey, 1998; Tcherkez, 2013; Hagemann; Bauwe, 2016).

A fotorrespiração é um processo metabólico em que, devido ao fechamento estomático, ocorre a oxigenação da molécula de ribulose-1,5-bifosfato (RuBP) pela Ribulose-Bifosfato Carboxilase/Oxigenase (RuBisCO), ao invés da carboxilação, gerando um 3-fosfoglicerato (3PG), que seguirá o metabolismo normal, e outra molécula de 2-fosfoglicolato (2PG) (Pick et al., 2013; Foyer et al., 2009; Hagemann; Bauwe, 2016; Stirbert et al., 2020). A molécula de PG para que seja reciclada novamente a RuBP, é levada a rota de fotorrespiração, onde a molécula de PG irá para o peroxissomo, na forma de glicolato, onde será oxidada pela Glicolato Oxidase (GLO/GOX) formando glioxilato e peróxido de hidrogênio, seguido pela conversão em glicina (Gly) ainda no peroxissomos (Hagemann; Bauwe, 2016).

A GLO é uma enzima oxidante de α-hidroxiácido flavina mononucleotídeo (FMN)-dependente encontrada tanto em plantas como em animais, pertencente à família

enzimas flavoproteínas oxidases (Figura C), onde a molécula de glicolato é oxidada pela porção de FMN da enzima, e reoxidada formando peróxido de hidrogênio (Foyer et al., 2009; Rojas et al., 2012; Yang et al., 2018; Liu et al., 2018;). GOX é responsável por cerca de 70% das espécies reativas de oxigênio (ROS) gerada durante a fotorrespiração no peroxissomos, apresentando um papel central no processo fotorrespiratório e em condições de estresse ambiental (Foyer et al., 2009). Para além desse processo metabólico, a glicolato oxidase possui um papel importante para o mecanismo de sinalização celular, principalmente na defesa contra patógenos (Yang et al., 2019).

Tendo em vista que a produção e depleção de ROS é vital para os estágios iniciais da infecção, já que influencia como a resposta da planta se dará e a sua velocidade (Li *et al*., 2021; Li *et al*., 2023). Para tal, o entendimento do aparato redox é chave para compreender como os organismos vegetais respondem a infecção por patógenos e como essas são moduladas. Entre as espécies reativas mais importantes para a resposta a estresse, o H_2O_2 já foi relatado sendo um importante mensageiro celular na rota relacionada a espécies reativas de oxigênio, tendo em vista sua estabilidade maior que as das outras formas de ROS e maior permeabilidade em relação as membranas celulares (Costa *et al*, 2010; Cui *et al*., 2016). Em estudos utilizando abordagens de proteômica em plantas de *V. unguiculata* usando plantas resistentes para o CPSMV, demonstraram nas primeiras horas após a infecção com o patógeno, um aumento na presença das proteínas homologas a GLO, isso para os dois primeiros dias após a infecção, no caso de 6 dias depois não foi observado mudanças (Varela et al., 2019). Outro trabalho usando *Nicotiana bethamiana* demonstrou ainda uma interação direta e física entre o vírus do mosaico estriado da cevada (BSMV) e a proteína GOX em folhas e a importância dessa proteína no balanço dessa espécie reativa de oxigênio e a resistência ao patógeno (Yang et al., 2018). Onde a proteína γb ao interagir com a GLO, diminuiu expressivamente o conteúdo de peróxido de hidrogênio, permitindo a infecção vírus (Yang et al., 2018). Com algo semelhante tendo sido demonstrado previamente para *Arabidopsis thaliana*, infectado com a bactéria *Pseudomonas syringae*, e *N. bethamiana*, com o vírus TRV (*Tobacco rattle virus*; vírus do chocalho do tabaco), onde foi reforçada a importância de GOX como uma fonte de H_2O_2 e na resposta tanto gene-gene ou não relacionado ao hospedeiro (Rojas et al., 2012).

Figura C. Principais locais de produção de H2O2 em células fotossintéticas. GO, glicolato oxidase. 3PGA, 3-fosfoglicerato. POX, peroxidase. RuBisCO, ribulose 1,5-bisfosfato carboxilase/oxigenase. RuBP, ribulose 1,5-bisfosfato. SOD, superóxido dismutase. XO,xantina oxidase.

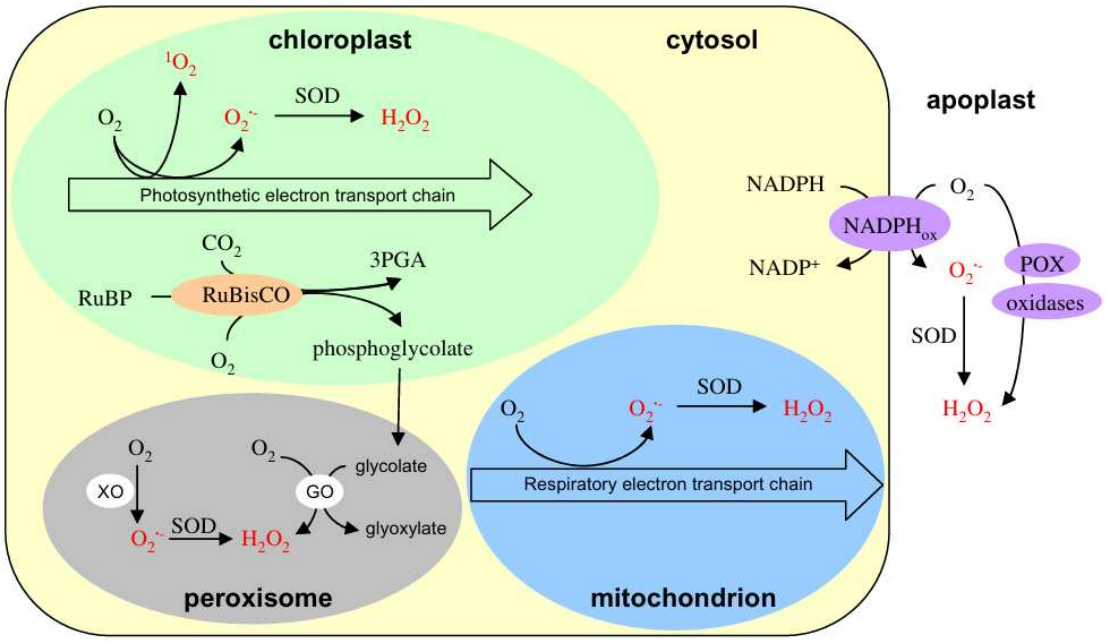

Fonte: (Mhamdi et al., 2010)

Entretanto, como todas as formas de espécies reativas, sua superprodução ou então a manutenção prolongada pode acabar sendo prejudicial para o indivíduo e seu funcionamento, tendo em vista a ocorrência de danos celulares, que a depender do nível, pode levar a morte celular (Wingler *et al.*, 2000; Gechev *et al.*, 2006). Assim, na região peroxissomal de forma antagônica com a glicolato oxidase há enzima Catalase (CAT), bem conhecida e descrita pelo seu papel antioxidante na quebra do peróxido de hidrogênio em água e oxigênio, visando minimizar os níveis dessa ROS nas células (Li et al., 2023; Riseh et al., 2024). Dessa forma, a CAT é uma enzima de extrema importância junto com a glicolato oxidase no peroxissomo, tendo em vista que a resposta a patógenos está intimamente ligada aos níveis de espécies reativas de oxigênio produzidas, e sua homeostase ao ponto de não danificar as células e atuarem como moléculas de sinalização celular (Guan; Scandalios, 2000; Foyer et al., 2009). Ademais, plantas de *N. bethamiana* demonstraram resistência ao vírus do mosaico do tabaco (TMV; *Tobacco Mosaic Virus*) após a superexpressão das cópias de CAT nas fases iniciais de infecção, relacionado a

diminuição do conteúdo de ROS e peróxido lipídios, permitindo a manutenção dos fotossistemas, além de um *crosstalk* com a rota de síntese de ácido salicílico (Huang et al., 2023).

Figura D. Um modelo de troca dinâmica para a associação-dissociação de glicolato oxidase e catalase em plantas. Onde há um mecanismo de canalização de substrato, quando o complexo GLO e CAT for dissociado, com o produto H_2O_2 sendo aumentado no meio em massa. Supõe-se que as difusões de glicolato (GCL) e H_2O_2 sejam direcionais.

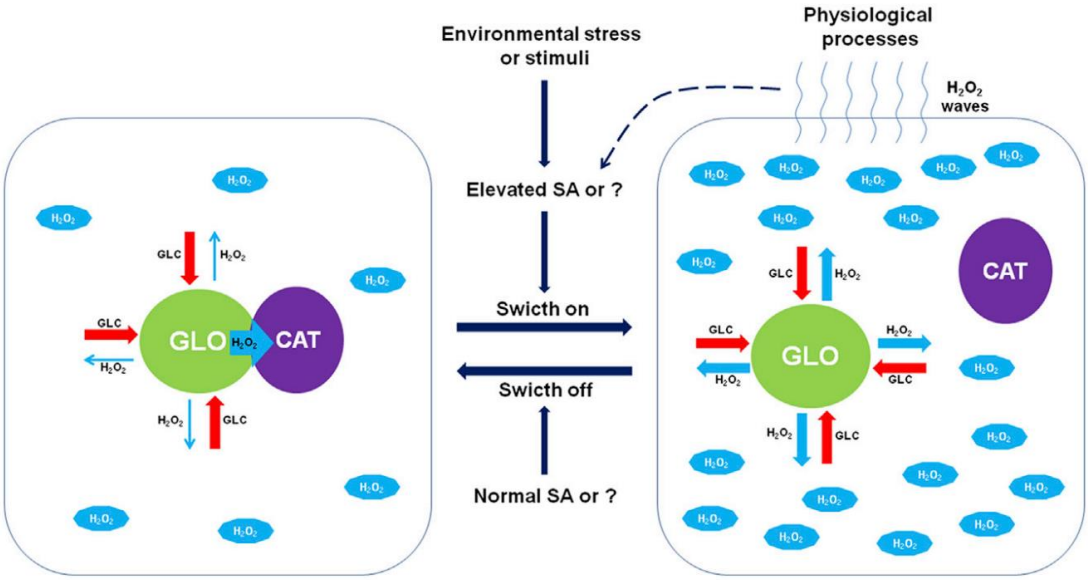

Fonte: (Zhang et al., 2016)

Como verificado na literatura, ambas as proteínas, GOX e CAT, possuem um papel chave na resposta a patógenos nas primeiras horas após o início do processo de infecção por agentes patogênicos (Li et al., 2023). Sendo essa interação ocorrendo de forma física demonstrado por Zhang e colaboradores (2016), onde em situações normais há um complexo formado entre GLO e CAT, o que modula uma menor produção de peróxido de hidrogênio (Figura D), mas sob algum estresse ou estímulo pode haver a dissociação do complexo e aumentando os níveis de H_2O_2 peroxissomal. Essa interação permitiria então o mecanismo já conhecido nos organismos vegetais a resposta a insetos e vírus, que seriam as ondas de peróxido de hidrogênio (*H_2O_2 waves*), que poderia estar relacionado a rota de síntese de ácido salicílico, comum na rota de resposta a patógenos (Zhang *et al.*, 2016). E um trabalho recente do mesmo grupo demonstrou uma relação

entre a formação de peróxido de hidrogênio e o complexo GLO-CAT, onde os canais de Ca^{+2} peroxissomais durante dano físico poderiam estar regulando a dissociação para uma resposta rápida com as ondas de peróxidos (Li et al., 2023). Assim, um mecanismo semelhante podendo ocorrer nas espécies vegetais durante a infecção por patógenos.

2 OBJETIVOS

2.1 Objetivo geral

Avaliar o papel das famílias de enzimas Glicolato Oxidase (GOX) e Catalase (CAT) de cultivares resistentes e susceptíveis de *Vigna unguiculata* [L.] Walp. durante a infecção pelo CPSMV.

2.2 Objetivos específicos

- Analisar o padrão de expressão dos genes de *VuGOX1*, *VuGOX2* e *VuGOX3*, durante tempos diferentes de inoculação com o vírus do mosaico severo do caupi (16 horas, 2 dias e 7 dias) em tecido foliar;
- Quantificar e comparar a atividade total e por cinética, dos cultivares susceptível e resistente, de Catalase por ensaios de atividade enzimática durante os tempos de coleta após infecção pelo patógeno CPSMV (16 horas, 2 dias e 7 dias);
- Avaliar e caracterizar a presença das cópias génicas de CAT (*VuCATa*; *VuCATb*; *VuCATc*) e sua expressão em tecidos foliares durante tempos diferentes de inoculação com o vírus do mosaico severo do caupi (16 horas, 2 dias e 7 dias) em cultivares resistentes e susceptíveis ao patógeno;
- Quantificação de peróxido de hidrogênio em tecido foliar durante tempos diferentes de inoculação com o vírus do mosaico severo do caupi (16 horas, 2 dias e 7 dias) em tecido foliar;
- Avaliar a resposta de cultivares resistente (Macaíbo) e susceptível (Pitiúba) a nível de transcrito e proteína, relacionado ao metabolismo redox, e correlacionar com suas respostas ao patógeno.

REFERÊNCIAS

ALLEN, D. J. (1983). The pathology of tropical food legumes: disease resistance in crop improvement.

ANDERSON, P. K.; CUNNINGHAM, A. A.; PATEL, N. G.; MORALES, F. J.; EPSTEIN, P. R.; DASZAK, P. Emerging infectious diseases of plants: pathogen pollution, climate change and agrotechnology drivers. **Trends in Ecology & Evolution**, v. 19, n. 10, p. 535-544, out. 2004. Disponível em: https://doi.org/10.1016/j.tree.2004.07.021. Acesso em: 23 de jan. de 2025.

BASTOS, E. A. **A cultura do feijão-caupi no Brasil**. Teresina: Embrapa Meio-Norte, 2017. 71 p. Disponível em: https://ainfo.cnptia.embrapa.br/digital/bitstream/item/156632/1/CulturaFeijaoCaupiBrasil.pdf . Acesso em: 11 mar. 2024. Acesso em: 23 de jan. de 2025.

BOOKER, H. M.; UMAHARAN, P.; MCDAVID, C. R. Effect of Cowpea severe mosaic virus on crop growth characteristics and yield of cowpea. **Plant disease**, v. 89, n. 5, p. 515-520, fev. 2005. Disponível em: https://doi.org/10.1094/PD-89-0515. Acesso em: 23 de jan. de 2025.

CARETTE, J. E.; van LENT, J.; MACFARLANE, S. A.; WELLINK, J.; van KAMMEN, A. Cowpea mosaic virus 32-and 60-kilodalton replication proteins target and change the morphology of endoplasmic reticulum membranes. **Journal of virology**, v. 76, n. 12, p. 6293-6301, jun. 2002. Disponível em: https://doi.org/10.1128/jvi.76.12.6293-6301.2002. Acesso em: 23 de jan. de 2025.

CARVALHO, M.; LINO-NETO, T.; ROSA, E.; CARNIDE, V. Cowpea: a legume crop for a challenging environment. **Journal of the Science of Food and Agriculture**, v. 97, n. 13, p. 4273-4284, out. 2017. Disponível em: 1 https://doi.org/10.1002/jsfa.8250. Acesso em: 23 de jan. de 2025.

CARVALHO, M.; CASTRO, I.; MOUTINHO-PEREIRA, J.; CORREIA, C.; EGEA-CORTINES, M.; MATOS, M.; ROSA, E.; CARNIDE, V.; LINO-NETO, T. Evaluating stress responses in cowpea under drought stress. **Journal of Plant Physiology**, v. 241, e153001, out. 2019. Disponível em: https://doi.org/10.1016/j.jplph.2019.153001. Acesso em: 23 de jan. de 2025.

CASSELL, M. E. (2011). *Bean Leaf Beetle: Impact of Leaf Feeding Injury on Snap Beans, Host Plant Choice and Role as a Vector of Bean Pod Mottle Virus in Virginia* (Doctoral dissertation, Virginia Tech).

CHEN, X.; BRUENING, G. Cloned DNA copies of cowpea severe mosaic virus genomic RNAs: Infectious transcripts and complete nucleotide sequence of RNA 1. **Virology**, v. 191, n. 2, p. 607–618, dez. 1992. Disponível em: https://doi.org/10.1016/0042-6822(92)90236-I. Acesso em: 23 de jan. de 2025.

CUI, L.-L.; LU, Y.-s.; LI, Y.; YANG, C.; PENG, X.-X. Overexpression of glycolate oxidase confers improved photosynthesis under high light and high temperature in Rice. **Frontiers in Plant Science**, v. 7, n. 1165, ago. 2016. Disponível em: https://doi.org/10.3389/fpls.2016.01165. Acesso em: 23 de jan. de 2025.

DURAIPANDIAN, M.; POORANI, K. E.; ABRIAMI, H.; ANUSHA, M. B. Vigna unguiculata (L.) Walp: A Strategic Crop for Nutritional Security, Well-being and Environmental Protection. In J. C. Jimenez-Lopez, A. Clemente (Eds.), Legumes – Volume 2. 2022.

FERREIRA-NETO, J. R. C.; BORGES, A. N. da C.; SILVA, M. D. da; MORAIS, D. A. de L.; BEZERRA-NETO, J. P.; BOURQUE, G.; KIDO, E. A.; BENKO-ISEPPON, A. M. The Cowpea Kinome: Genomic and Transcriptomic Analysis Under Biotic and Abiotic Stresses. **Frontiers in Plant Science**, v. 12, e667013, jun. 2021. Disponível em: https://doi.org/10.3389/fpls.2021.667013. Acesso em: 23 de jan. de 2025.

FOYER, C. H.; BLOOM, A. J.; QUEVAL, G.; NOCTOR, G. Photorespiratory Metabolism: Genes, Mutants, Energetics, and Redox Signaling. **Annual Review of Plant Biology**, v. 60, p. 455–484, jun. 2009. Disponível em: https://doi.org/10.1146/annurev.arplant.043008.091948. Acesso em: 23 de jan. de 2025.

FUCHS, M.; HILY, J.-M.; PETRZIK, K.; SANFAÇON, H.; THOMPSON, J. R.; van der VLUGT, R.; WETZEL, T.; ICTV Report Consortium. ICTV Virus Taxonomy Profile: *Secoviridae* 2022. **Journal of General Virology**, v. 103, n. 12, e001807, out. 2022. Disponível em: https://doi.org/10.1099/jgv.0.001807. Acesso em: 23 de jan. de 2025.

FULTON, J. P.; SCOTT, H. A. A Serogrouping Concept For Legume Comoviruses. **Phytopathology**, v. 69, n. 4, p. 305-306, fev. 1979. Disponível em: https://doi.org/10.1094/Phyto-69-305. Acesso em: 23 de jan. de 2025.

GECHEV, T. S.; van BREUSEGEM, F.; STONE, J. M.; DENEV, I.; LALOI, C. Reactive oxygen species as signals that modulate plant stress responses and programmed cell death. **Bioessays**, v. 28, n. 11, p. 1091–1101. Disponível em: https://doi.org/10.1002/bies.20493. Acesso em: 23 de jan. de 2025.

Goldbach, R. and Wellink, J. (1996) Comoviruses: molecular biology and replication. In: The Plant Viruses, Polyhedral Virions and Bipartite RNA Genomes, Vol. 5, pp. 35–76. Plenum Press, New York.

GOMES, A. M. F.; RODRIGUES, A. P.; ANTÓNIO, C.; RODRIGUES, A. M.; LEITÃO, A. E.; BATISTA-SANTOS, P.; NHANTUMBO, N.; MASSINGA, R.; RIBEIRO-BARROS, A. I.; RAMALHO, J. C. Drought response of cowpea (Vigna unguiculata (L.) Walp.) landraces at leaf physiological and metabolite profile levels. **Environmental and Experimental Botany**, v. 175, e104060, jul. 2020. Disponível em: https://doi.org/10.1016/j.envexpbot.2020.104060. Acesso em: 23 de jan. de 2025.

GONÇALVES, A.; GOUFO, P.; BARROS, A.; DOMÍNGUEZ-PERLES, R.; TRINDADE, H.; ROSA, E. A.; FERREIRA, L.; RODRIGUES, M. Cowpea (Vigna unguiculata L. Walp), a renewed multipurpose crop for a more sustainable agri-food system: nutritional advantages and constraints. **Journal of the Science of Food and Agriculture**, v. 96, n. 9, p. 2941-2951, jan. 2016. Disponível em: https://doi.org/10.1002/jsfa.7644. Acesso em: 23 de jan. de 2025.

GUAN, L. M.; SCANDALIOS, J. G. Hydrogen peroxide-mediated catalase gene expression in response to wounding. **Free Radical Biology and Medicine**, v. 28, n. 8, p. 1182-1190, abr. 2000. Disponível em: https://doi.org/10.1016/S0891-5849(00)00212-4. Acesso em: 23 de jan. de 2025.

HAGEMANN, M.; BAUWE, H. Photorespiration and the potential to improve photosynthesis. **Current opinion in chemical biology**, v. 35, p. 109-116, set. 2016. Disponível em: https://doi.org/10.1016/j.cbpa.2016.09.014. Acesso em: 23 de jan. de 2025.

HALL, A.E.; CISSE, N.; THIAW, S.; ELAWAD, H. O. A.; EHLERS, J. D.; ISMAIL, A. M.; FERY, R. L.; ROBERTS, P. A.; KITCH, L. W.; MURDOCK, L. L.; BOUKAR, O.; PHILLIPS, R. D.; MCWATTERS, K. H. Development of cowpea cultivars and germplasm by the Bean/Cowpea CRSP. **Field Crops Research**, v. 82, n. 2-3, p. 103-134, mai. 2003. Disponível em: https://doi.org/10.1016/S0378-4290(03)00033-9. Acesso em: 23 de jan. de 2025.

HUANG, W.; JIAO, B.; JI, C.; PENG, Q.; ZHOU, J.; YANG, Y.; XI, D. Catalases mediate tobacco resistance to virus infection through crosstalk between salicylic acid and auxin signaling pathways. **Physiologia Plantarum,** v. 175, n. 5, e14012, fev. 2023. Disponível em: https://doi.org/10.1111/ppl.14012. Acesso em: 23 de jan. de 2025.

ICTV International Committee on Taxonomy of Viruses: ICTV. https://ictv.global/taxonomy/ Acessso em: 16 de fev. de 2025

JAYAWARDHANE, J.; GOYALI, J. C.; ZAFARI, S.; IGAMBERDIEV, A. U. The Response of Cowpea (*Vigna unguiculata*) Plants to Three Abiotic Stresses Applied with Increasing Intensity: Hypoxia, Salinity, and Water Deficit. **Metabolites**, v. 12, n. 1, ´p. 38, jan. 2022. Disponível em: https://doi.org/10.3390/metabo12010038. Acesso em: 23 de jan. de 2025.

KAREEM, K. T.; TAIWO, M. A. Interactions of viruses in cowpea: effects on growth and yield parameters. **Virology Journal**, v. 4, n. 15, fev. 2007. Disponível em: https://doi.org/10.1186/1743-422X-4-15. Acesso em: 23 de jan. de 2025.

KITAJIMA, E.W. An annotated list of plant viruses and viroids described in Brazil (1926-2018). **Biota Neotropica**, v. 20, n. 2, e20190932, jan. 2020. Disponível em: https://doi.org/10.1590/1676-0611-BN-2019-0932. Acesso em: 23 de jan. de 2025.

LI, X.; CHEN, L.; ZENG, X.; WU, K.; HUANG, J.; LIAO, M.; XI, Y.; ZHU, G.; ZHENG, X.; HOU, X.; ZHANG, Z.; PENG, X. Wounding induces a peroxisomal H2O2 decrease via glycolate oxidase-catalase switch dependent on glutamate receptor-like channel-supported Ca2+ signaling in plants. **The Plant Journal**, v. 116, p. 1325-1341, ago. 2023. Disponível em: https://doi.org/10.1111/tpj.16427. Acesso em: 23 de jan. de 2025.

LI, X.; LIAO, M.; HUANG, J.; XU, Z.; LIN, Z.; YE, N.; ZHANG, Z.; PENG, X. Glycolate oxidase-dependent H2O2 production regulates IAA biosynthesis in rice. **BMC Plant Biology**, v. 21, n. 336, jun. 2021. Disponível em: https://doi.org/10.1186/s12870-021-03112-4. Acesso em: 23 de jan. de 2025.

LIMA, J. A. A.; NASCIMENTO, A. K.Q. D.; SILVA, A. K. F. D.; AARAGÃO, M. D. L. Biological stability of a strain of Cowpea severe mosaic virus over 20 years. **Revista Ciência Agronômica**, v. 43, n. 1, p. 105–111, jan-mar. 2012. Disponível em: https://doi.org/10.1590/S1806-66902012000100013. Acesso em: 23 de jan. de 2025.

MARTINS, L. M. V.; XAVIER, G. R.; RANGEL, F. W.; RIBEIRO, J. R. A.; NEVES, M. C. P.; MORGADO, L. B.; RUMJANEK, N. G. Contribution of biological nitrogen fixation to cowpea: a strategy for improving grain yield in the semi-arid region of Brazil. **Biology and fertility of soils**, v. 38, p. 333-339, jul. 2003. Disponível em: https://www.alice.cnptia.embrapa.br/bitstream/doc/152219/1/Separata01302.pdf. Acesso em: 23 de jan. de 2025.

NAWAZ, M.; SUN, J.; SHABBIR, S.; KHATTAK, W. A.; REN, G.; NIE, X.; BO, Y.; JAVED, Q.; DU, D.; SONNE, C. A review of plants strategies to resist biotic and abiotic environmental stressors. **Science of The Total Environment**, v. 900, e165832, nov. 2023. Disponível em: https://doi.org/10.1016/j.scitotenv.2023.165832. Acesso em: 23 de jan. de 2025.

SOUZA, P. F. N.; OLIVEIRA, J. T. A.; VASCONCELOS, I. M.; MAGALHÃES, V. G.; SILVA, F. D. A.; SILVA, R. G. G.; OLIVEIRA, K. S.; FRANCO, O. L.; SILVEIRA, J. A. G.; CARVALHO, F. E. L. H2O2 Accumulation, Host Cell Death and Differential Levels of Proteins Related to Photosynthesis, Redox Homeostasis, and Required for Viral Replication Explain the Resistance of EMS-Mutagenized Cowpea to Cowpea Severe Mosaic Virus. **Journal of Plant Physiology**, v. 245, e153110, fev. 2020. Disponível em: https://doi.org/10.1016/j.jplph.2019.153110. Acesso em: 23 de jan. de 2025.

OMOMOWO, O. I.; BABALOLA, O. O. Constraints and prospects of improving cowpea productivity to ensure food, nutritional security and environmental sustainability. **Frontiers in Plant Science**, v. 12, e751731, out. 2021. Disponível em: https://doi.org/10.3389/fpls.2021.751731. Acesso em: 23 de jan. de 2025.

PEREIRA, E. J.; CARVALHO, L. M.; DELLAMORA-ORTIZ, G. M.; CARDOSO, F. S.; CARVALHO, J. L.; VIANA, D. S.; FREITAS, S. C.; ROCHA, M. M. Effects of cooking methods on the iron and zinc contents in cowpea (Vigna unguiculata) to combat nutritional deficiencies in Brazil. **Food & Nutrition Research**, v. 58, e20694, fev. 2014. Disponível em: https://doi.org/10.3402/fnr.v58.20694. Acesso em: 23 de jan. de 2025.

PETERS, S. A.; VERVER, J.; NOLLEN, E. A.; van LENT, J. W.; WELLINK, J.; van KAMMEN, A. The NTP-binding Motif in Cowpea Mosaic Virus B Polyprotein is Essential for Viral Replication. **Journal of General Virology**, v. 75, n. 11, p. 3167-3176, nov. 1994. Disponível em: https://doi.org/10.1099/0022-1317-75-11-3167. Acesso em: 23 de jan. de 2025.

POUWELS, J.; CARETTE, J. E.; van LENT, J.; WELLINK, J. Cowpea mosaic virus: effects on host cell processes. **Molecular Plant Pathology**, v. 3, n. 6, p. 411-418, out. 2002. Disponível em: https://doi.org/10.1046/j.1364-3703.2002.00135.x. Acesso em: 23 de jan. de 2025.

RAHEJA, A. K.; LELEJI, O. I. An aphid-borne virus disease of irrigated cowpea in Northern Nigeria. **Plant Disease Reporter**, v. 58, n. 12, p. 1080-1084, jan. 1975.

RISEH, R. S.; FATHI, F.; VATANKHAH, M.; KENNEDY, J. F. Catalase-associated immune responses in plant-microbe interactions: A review. **International Journal of Biological Macromolecules**, v. 280, e135859, nov. 2024. Disponível em: https://doi.org/10.1016/j.ijbiomac.2024.135859. Acesso em: 23 de jan. de 2025.

ROJAS, C. M.; SENTHIL-KUMAR, M.; WANG, K.; RYU, C. M.; KAUNDAL, A.; MYSORE, K. S. Glycolate Oxidase Modulates Reactive Oxygen Species–Mediated Signal Transduction during Nonhost Resistance in *Nicotiana benthamiana* and *Arabidopsis*. **The Plant Cell**, v. 24, n. 1, p. 336-352, jan. 2012. Disponível em: https://doi.org/10.1105/tpc.111.093245. Acesso em: 23 de jan. de 2025.

SANFAÇON, H.; WELLINK, J.; LE GALL, O.; KARASEV, A.; van der VLUGT, R.; WETZEL, T. Secoviridae: a proposed family of plant viruses within the order *Picornavirales* that combines the families *Sequiviridae* and *Comoviridae*, the unassigned genera *Cheravirus* and *Sadwavirus*, and the proposed genus Torradovirus. **Archives of Virology**, v. 154, p. 899-907, abr. 2009. Disponível em: https://doi.org/10.1007/s00705-009-0367-z. Acesso em: 23 de jan. de 2025.

SHARKEY, T. D. Estimating the rate of photorespiration in leaves. **Physiologia Plantarum**, v. 73, n. 1, p. 147-152, mai. 1988. Disponível em: https://doi.org/10.1111/j.1399-3054.1988.tb09205.x. Acesso em: 23 de jan. de 2025.

SHOYINKA, S. A.; THOTTAPPILLY, G.; ADEBAYO, G. G.. ANNO-NYAKO, F. O. Survey on cowpea virus incidence and distribution in Nigeria**. International Journal of Pest Management**, v. 43, n. 2, p. 127-132, 1997. Disponível em: https://doi.org/10.1080/096708797228816. Acesso em: 23 de jan. de 2025.

SILVEIRA, J. A. G. D.; COSTA, R. C. L. D.; OLIVEIRA, J. T. A. DROUGHT-INDUCED EFFECTS AND RECOVERY OF NITRATE ASSIMILATION AND NODULE ACTIVITY IN COWPEA PLANTS INOCULATED WITH *BRADYRHIZOBIUM* SPP. UNDER MODERATE NITRATE LEVEL. **Brazilian Journal of microbiology**, v. 32, n. 3, p. 187-194, out. 2001. Disponível em: https://doi.org/10.1590/S1517-83822001000300005. Acesso em: 23 de jan. de 2025.

SOUZA, P. F. N.; SILVA, F. D. A.; CARVALHO, F. E. L.; SILVEIRA, J. A. G.; VASCONCELOS, I. M.; OLIVEIRA, J. T. A. Photosynthetic and biochemical mechanisms of an EMS-mutagenized cowpea associated with its resistance to *cowpea severe mosaic virus*. **Plant Cell Reports**, v. 36, p. 219-234, nov. 2016. Disponível em: https://doi.org/10.1007/s00299-016-2074-z. Acesso em: 23 de jan. de 2025.

STIRBET, A.; LAZÁR, D.; GUO, Y.; GOVINDJEE, G. Photosynthesis: basics, history and modelling. **Annals of Botany**, v. 126, n. 4, p. 511-537, set. 2020. Disponível em: https://doi.org/10.1093/aob/mcz171. Acesso em: 23 de jan. de 2025.

STUKENBROCK, E. H.; MCDONALD, B. A. The origins of plant pathogens in agroecosystems. **Annual Review of Phytopathology**, v. 46, p. 75-100, set. 2008. Disponível em: https://doi.org/10.1146/annurev.phyto.010708.154114.

TCHERKEZ, G. Is the recovery of (photo) respiratory CO2 and intermediates minimal? **New Phytologist**, v 198, n. 2, p. 334-338, dez. 2012. Disponível em: https://doi.org/10.1111/nph.12101. Acesso em: 23 de jan. de 2025.

TEIXEIRA, K. J. M. L.; CASCARDO, R. de S.; LEAL, L. L.; ZERBINI, F. M.; BESERRA JR., J. E. A. First complete genome sequence of an isolate of cowpea severe mosaic virus from South America. **Virus Genes**, v. 57, n. 2, p. 238-241, fev.

2021. Disponível em: https://doi.org/10.1007/s11262-021-01831-2. Acesso em: 23 de jan. de 2025.

THOMPSON, J. R.; DASGUPTA, I.; FUCHS, M.; IWANAMI, T.; KARASEV, A. V.; PETRZIK, K.; SANFAÇON, H.; TZANETAKIS, I.; van der VLUGT, R.; WETZEL, T.; YOSHIKAWA, N.; ICTV REPORT CONSORTIUM. ICTV virus taxonomy profile: *Secoviridae*. **Journal of General Virology**, v. 98, n. 4, p. 529-531, abr. 2017. Disponível em: https://doi.org/10.1099/jgv.0.000779. Acesso em: 23 de jan. de 2025.

TREBICKI, P. Climate change and plant virus epidemiology. **Virus Research**, v. 286, e198059, set. 2020. Disponível em: https://doi.org/10.1016/j.virusres.2020.198059. Acesso em: 23 de jan. de 2025.

VARELA, A. L. N.; OLIVEIRA, J. T. A.; KOMATSU, S.; SILVA, R. G. G.; MARTINS, T. F.; LOBO, A. K. M.; VASCONCELOS, I. M.; CARVALHO, F. E. L.; SILVEIRA, J. A. G. A resistant cowpea (*Vigna unguiculata* [L.] Walp.) genotype became susceptible to cowpea severe mosaic virus (CPSMV) after exposure to salt stress. **Journal of Proteomics**, v. 194, p. 200-217, mar. 2019. Disponível em: https://doi.org/10.1016/j.jprot.2018.11.015. Acesso em: 23 de jan. de 2025.

WINGLER, A.; LEA, P. J.; QUICK, W. P.; LEEGOOD, R. C. Photorespiration: metabolic pathways and their role in stress protection. **Philosophical Transactions of the Royal Society of London. Series B: Biological Sciences**, v. 355, n. 1402, p. 1517-1529, out. 2020. Disponível em: https://doi.org/10.1098/rstb.2000.0712. Acesso em: 23 de jan. de 2025.

YANG, M.; LI, Z.; ZHANG, K.; ZHANG, X.; ZHANG, Y.; WANG, X.; HAN, C.; YU, J.; XU, K.; LI, D. *Barley Stripe Mosaic Virus* γb Interacts with Glycolate Oxidase and Inhibits Peroxisomal ROS Production to Facilitate Virus Infection. **Molecular Plant**, v. 11, n. 2, p. 338-341, fev. 2018. Disponível em: https://doi.org/10.1016/j.molp.2017.10.007. Acesso em: 23 de jan. de 2025.

ZHANG, Y.; XU, J.; LI, R.; GE, Y.; LI, Y.; LI, R. Plants' response to abiotic stress: Mechanisms and strategies. **International Journal of Molecular Sciences**, v. 24, n. 13, e10915, jun. 2023. Disponível em: https://doi.org/10.3390/ijms241310915. Acesso em: 23 de jan. de 2025.

ZHANG, Z.; LI, X.; CUI, L.; MENG, S.; YE, N.; PENG, X. Catalytic and functional aspects of different isozymes of glycolate oxidase in rice. **BMC Plant Biology**, v. 17, n. 135, ago. 2017. Disponível em: https:// doi.org/10.1186/s12870-017-1084-5. Acesso em: 23 de jan. de 2025.

ZHANG, Z.; XU, Y.; XIE, Z.; LI, X.; HE, Z. H.; PENG, X. X. Association–dissociation of glycolate oxidase with catalase in rice: a potential switch to modulate intracellular H2O2 levels. **Molecular Plant**, v. 9, n. 5, p. 737-748, mai. 2016. Disponível em: https://doi.org/10.1016/j.molp.2016.02.002. Acesso em: 23 de jan. de 2025.

ZHAO, L.; FENG, C.; WU, K.; CHEN, W.; CHEN, Y.; HAO, X.; WU, Y. Advances and prospects in biogenic substances against plant virus: a review. **Pesticide Biochemistry and Physiology**, v. 135, p. 15–26, jan. 2017. Disponível em: https://doi.org/10.1016/j.pestbp.2016.07.003. Acesso em: 23 de jan. de 2025.

3 MANUSCRITO

Functional role of the Glycolate Oxidase (GOX) and Catalase (CAT) enzyme families in the response to *Cowpea Severe Mosaic Virus* in *Vigna unguiculata* [L.] Walp

Victor Breno Faustino Bezerra[1], João Victor Dourado Alves Brito[1], Gabriela Oliveira Matos[1], Lorenna Maria Neves Freitas[1], Murilo Siqueira Alves[1*]

[1] Departamento de Bioquímica e Biologia Molecular, Universidade Federal do Ceará, Avenida Humberto Monte S/N, Campus do Pici, Fortaleza, CE, 60440-900, Brazil

[*]Corresponding author: murilo.alves@ufc.br

ABSTRACT

With the increase in food shortages and nutritional deficiencies, the choice of alternative crops with relevant characteristics is important. *Vigna unguiculata* L. is therefore a crop of great interest. However, cowpeas are still susceptible to some pathogens, such as the *CowPea Severe Mosaic Virus* (CPSMV). Under adverse conditions, such as infection by pathogens, one of the initial mechanisms for the stress response involves the production of reactive oxygen species. One of these molecules is hydrogen peroxide, which has its highest production rate related to Glycolate Oxidase (GOX), an enzyme in the photorespiration process, but like all reactive species, its production and consumption must be finely balanced, so there is the peroxisomal enzyme Catalase (CAT), responsible for this control during a stress phenomenon. The aim of this study was therefore to analyse the expression of GOX and CAT gene copies, at transcript and activity level, in response to CPSMV. To this end, the plant specimens were inoculated with CPSMV at three time points (16 hours, 48 hours and 144 hours). Analyses of catalase enzyme activity showed differences between the cultivars only in the initial hours (16h), in the control conditions of inoculated Pitiúba and Mock, possibly related to the initial response to the pathogen. In addition, analyses using DAB (3,3'-Diaminobenzidine) staining, MDA (Malonaldehyde) and peroxide content were used to determine the degree of oxidative stress, again with differences only between Pitiúba Mock and inoculated at 16 and 48 hours. In addition, the expression data showed differences mainly in the VuGOX1 gene in the Macaíbo cultivar, whose expression was induced during infection compared to the Mock. While VuGOX2 was the gene with the highest abundance at transcript level, showing differences between the cultivars at times of 16 and 144h, with reduced expression in inoculated Pitiúba compared to Mock 144h. Analysis of *cis*-elements showed regions that corroborate points raised in the discussion, mainly related to the pathogen response route and the synthesis of salicylic acid (SA). Thus, it is hoped that the results found will help breeding programmes and understanding of the resistance phenomenon.

Keywords: Photorespiration; *Comovirus*; Glicolate Oxidase; Catalase; Resistence; Cowpea Severe Mosaic Virus.

3.1 INTRODUCTION

The cowpea plant (*Vigna unguiculata* [L.] Walp.) is one of the most important agronomic crops regionally in tropical and subtropical areas, due to its ecological and nutritional impact (Gonçalves *et al.*, 2016; Duraipandian *et al.*, 2022). However, cowpea plants throughout the world, besides being affected by salinity or other types of abiotic stress, suffers mainly due to pathogens. Among all those that infect cowpea, the *Cowpea Severe Mosaic Virus* (CPSMV) is the major pathogen affecting productivity (Booker; McDavid, 2005; Bastos, 2017; Carvalho *et al.*, 2019; Kitajima *et al.*, 2020; Gomes *et al.*, 2022; Jayawardhane *et al.*, 2022).

The CPSMV is a *Comovirus* from the Secorovidae which has the Fabaceae members as its main host, being characterized by its genetic material as a single strand RNA (ssRNA) with a positive sense (+), and bipartite, with two RNA molecules (RNA1 and RNA2) (Thompson *et al.*, 2017; Walker *et al.*, 2020; Pouwels *et al.*, 2020; Fuchs *et al.*, 2022). Infections with CPSMV are responsible for 85% of production loss in cowpea plants, due to its symptoms, such as leaf reduction, chlorotic leaves with mosaic pattern, leaf crinkling, and necrosis, leading to photosynthetic loss which directly affects yield; (Booker; McDavid, 2005; Lima *et al.*, 2012; Souza *et al.*, 2017; Varela *et al.*, 2018).

When infected by a pathogen, plants normally trigger diverse types of mechanisms, such as differential expression of pathogens-related genes, changes in the metabolic and ion flux pathways, and the production and balance of reactive oxygen species (ROS) (Mandadi; Scholthof, 2013; Pandey *et al.*, 2015). ROS production is a key factor in a wide range of responses to a plethora of stimuli, such as viral infection, since these molecules act as an important signal in plant systems (Averyanov, 2009; Bacete; Mélida; Molina, 2017; Li *et al.*, 2023; Riseh; Fathi; Vatankhak; Kennedy, 2024). Among all ROS, hydrogen peroxide (H_2O_2) is a key molecule, due to its stability and capability to pass through cell walls, playing an important role in pathogen response (Costa *et al.*, 2010; Cui *et al.*, 2016). Since mainly H_2O_2 and other types of ROS lead plant cells to respond by expressing pathogen-related proteins (PR-proteins) which leads plants to hypersensitive response (HR), a key mechanism to stop pathogen from spreading to other healthy cells and turning the infection systemic, mainly due to programmed cell death (PCD) (Mandadi; Scholthof, 2013; Riseh *et al.*, 2024). Which in some cases could lead to systemic acquired? resistance (SAR).

Thus, due to its importance, plants along the evolutive course-maintained mechanism that is able to finely regulate the levels of ROS, mainly in the H_2O_2 homeostasis, where among the enzymatic apparatus the Glycolate Oxidase (GLO/GO) is responsible for converting the glycolate, under photorespiration, to glyoxylate, for the recycle to glyceradehyde-3-phosphate (G3P) to return to the Calvin-Benson Cycle (Foyer et al., 2009; Liu et al., 2018).

GOX is responsible for more than 70% of hydrogen peroxide production in the cell, thus reaffirming its importance (Foyer et al., 2009; Zhang et al., 2017). However, the production of ROS without regulation could leave cells to oxidative stress, thus other enzyme that works antagonistically with GLO is Catalase (CAT), which acts depleting H_2O_2 and forming water and oxygen as a final product (Li et al., 2013; Riseh et al., 2024). Previous works has shown a possible GOX-CAT association-dissociation mechanism (GC switch) responsible to modulate intracellular hydrogen peroxide levels, where environmental or stimuli (Zhang et al., 2016). With the GC switch being related to plant response by regulating H_2O_2 waves involved in plant systemic response to abiotic/biotic stress (Li et al., 2023). And previous works using contrasting *V. unguiculata* cultivars showed an increase of hydrogen peroxide with plants infected with CPSMV and combined with salinity, as well as the increase GLO and CAT using proteomics approach (Varela et al. 2019).

Genome-wide analysis in cowpea plants identified three genes of GOX in its genome, *VuGOX1* (*Vigun01g052400*), *VuGOX2* (*Vigun03g162000*) and V*uGOX3* (*VigunL052501*), where the two first genes are the most expressed in leaves, where the *VuGOX3* is expressed in radicular portion (Roque et al., 2023). And catalase has also three genes in cowpea genome, being *VuCATa* (*Vigun09g260100*), *VuCATb* (*Vigun08g001400*) e *VuCATc* (*Vigun05g264800*) (Goodstein et al., 2012). Thus, due to the importance of the interaction between catalase and glycolate oxidase for the hydrogen peroxide levels modulations, *V. unguiculata* was chosen as model to understand under CPSMV inoculation, using two contrasting cultivars, the role of GOX and CAT copies after infection response.

3.2 MATERIAL AND METHODS

3.2.1 Cultivars growth conditions and CPSMV inoculation

The Pitiúba, described as susceptible to CPSMV virus, and Macaibo cultivars were provided by the Laboratório de Análise de Sementes (LASA), from Universidade Federal do Ceará (UFC), which were used to carry out the experiments and analysis. The seed were germinated in 2,5 L pots filled with a substrate composed of 1: 1 soil: vermiculite. During the growth period cowpea plants were maintained in greenhouse conditions, with a photoperiod of 12h/12h (light/dark), with relative humidity of 70% and medium temperature of 35/37°C.

For the treatments 2 groups were formed for each collection time, on being the mock, where the plants were not inoculated with the virus, and inoculated, with each group containing 5 biological replicates, having a factorial design of 2 cultivars x 5 replicates x 2 treatments = 60 plants at the total. The inoculation with CPSMV were performed with plants as with the third trifoliate leaves fully expanded (V4), and the samples were collected after 16h, 2 days (48h) and 7 days (144h) post inoculation (hpi), where the leaves tissues were maintained in liquid nitrogen and storage at 80ºC for further analysis. Thus, the treatments were nominated Mock of Pitiúba after 16h (Mock16-P) and Pitiúba inoculated after 16 (P-16), the same used for Macaibo genotype: Mock16-M and M-16. And the same nomenclature used for the other times, such as Mock48-P, P-48, Mock48-M and M-48, for 48h inoculation, and Mock144-P, P-144, Mock144-M and M-144, for 144h inoculation.

The inoculation with Cowpea Severe Mosaic Virus was performed as described by Texeira *et al.* (2023). Where 1,5g of inoculated leaves were grounded with the aid of a mortar and pistil using 10 mL of phosphate buffer 100 mM pH 7.0 with sodium sulfite 0,1% (m/v), and an abrasive (*carburudum*) added at the end of the process in a proportion of 1: 8. And for the negative control (*Mock)* plants the same process was performed but using heathy leaves.

3.2.2 Catalase (CAT) activity

Catalase activity was performed as described by Beers and Sizers (1952), with the adaptations of Queiroz *et al*. (2020). Thus, 100 mg of fresh mass was extracted with the aid of liquid nitrogen, mortar and pistil, and homogenised with 1,5 mL of cold phosphate buffer 100 mM pH 7.0 and maintained in ice in all further steps. After that, the samples were centrifuged at 12.000g at 4°C for 15 minutes, and the supernatant obtained transferred to a new tube. The enzymatic extract used for the assay, where assay tubes

containing 1290 uL of phosphate buffer 100 mM pH 7.0 at 37°C was added with 60 uL of hydrogen peroxide 60 mM, followed by vortex, and finally added 150 uL of the sample extract. The reads were performed in the wavelenght of λ = 240 nm during 1 minute at each 15 seconds. Catalase activity was expressed using the breakdown of hydrogen peroxide and expressed as H_2O_2.minute^{-1} fresh mass.

3.2.3 Hydrogen peroxide quantification in leaves tissue

For hydroperoxide quantification in leaf tissue the method used was performed as described by Velikova & Yordanov (2000). Approximately 100 mg of fresh mass of the leaf were homogenised with 1 mL of TCA 5% (m:v) with the aid of a mortar and a pistil, where the homogenised was centrifuged at 12.000 g for 20 min at 4°C. The obtained supernatant was used for the hydrogen peroxide quantification, by adding 100 uL in a solution of potassium iodate (KI) and phosphate buffer 100 mM pH 7.0, followed by vortex. All the reactions were performed in the dark and incubated for 15 minutes at room temperature. At the end the samples were read at 390 nm, with the absorption obtained was used to calculate the hydrogen peroxide concentration, by using a standard curve. And expressed as μmol H_2O_2 g^{-1} of fresh mass.

3.2.4 Dead cells detection in *Vigna unguiculata* leaves

For the detection of H_2O_2 accumulation, cowpea leaves were detached and incubated in DAB (3,3'-Diaminobenzidine) [4,67 mM DAB; 1% isopropanol (v/v); Triton 0,1% (v/v)], covered in aluminium, for 24 h. After that period, the leaves were incubated in whitening solution (ethanol: acetic acid: glycerol; 4: 1: 1) for 24 h, and at the end the leaved were incubated in water bath at 95°C until the solution evaporates.

3.2.5 Oxidative damage

The oxidative damage was assessed by measuring cell membrane damage and the content of malondialdehyde (MDA), a product of lipids peroxidation. MDA was quantified using the thiobarbituric acid reactive species (TBARS) method (Heath & Pack *et al*., 1986; Carvalho *et al*., 2019). Approximately 100 mg of fresh mass of leafs were homogenised with 1 mL of TCA 5% (m:v) with the aid of a mortar and a pistil. The homogenised obtained was centrifuged at 12.000g for 15 min at 4°C, and the supernatant obtained transferred to a new tube, where was added 500 uL of TBA 0,5% and 500 uL of TCA20% and incubated for 30 min at 95°C to accelerate the reaction. After the reaction

the samples were read in a spectrophotometer at the absorbance of 532 nm and 600 nm, where the MDA concentration was expressed as nM of MDA. g^{-1} Fresh Mass.

3.2.6 RNA extraction

For the RNA extraction 100 mg of leaf tissue was pulverized with the aid of liquid nitrogen, pistil, mortar and extracted with the Ribospin^{TM} vRD Kit (GeneAll) using microcolumns. Where 500 uL of VL Buffer were added to the leaf tissue, vortexed and incubated for 10 minutes at room temperature, and after that period centrifuged at 12.000 g for 1 minute at 25 °C, with the supernatant collected and transferred to a new microtube. The supernant was mixed with 700uL of the RBI buffer and homogenised and vortexed. After that 750uL of the supernatant was added to the microcolumns type IV and followed by centrifugation at 12.000 g for 30 seconds at 25°C, with the mobile phase discarded and the previous step repeated with the remain sample.

After this step, 500 uL of RBW buffer was added to the microcolumn type IV and centrifuge at 10.000 g for 30 seconds at 25°C, with the mobile discarded, and followed by the addition of 500 uL of RNW buffer as previously described. To remove the excess of the RNW buffer, the microcolumn was centrifuged one more time at 10.000 g for 1 min at 25°C.

The microcolumn was transferred to new nuclease free microtubes and added 30 uL of nuclease free water in the middle of the membrane and incubated for 1 minute, followed by a centrifugation at 10.000g for 1 min at 25°C. Where the RNA samples were storage at -80°C for further analysis.

Due to Ribospin^{TM} vRD Kit (GeneAll) RNA lower extraction yields other extraction, to extract 2ug of RNA, TRIzol extraction was performed using 100mg tissue from each sample grounded using a mortar and a pestle (cooled in liquid nitrogen). The obtained powder was transferred to a tube (RNAse-free) and then 1 mL of TRIzol was added. Samples was incubated for 5 min at 25 °C for complete dissociation of the nucleoprotein complexes. After incubation, 0.2 mL of chloroform is added to the mixture and shaken vigorously for 15 s. Afterwards, it is centrifuged for 15 min, 12 000 x g, 4 °C and the RNA present in the aqueous phase is transferred to a new tube. The RNA is precipitated by adding 0.5 mL isopropanol and kept on ice for 10 min. It is then centrifuged for 10 min, 12 000 x g, 4 °C. The supernatant is discarded and the RNA pellet washed with 1 mL of 75% (v/v) Ethanol and vortexed. The sample will be centrifuged

for 5 min, 7,500 x g, 4 °C, the supernatant discarded. The resulting RNA pellet dried at 25 °C for ethanol evaporation. The pellet obtained was resuspended with 25 uL of deionized water (RNase-free) and stored at -80 °C.

3.2.7 cDNA synthesis and quantitative PCR analysis

The cDNA synthetized was obtained using 2 ug of total RNA, oligo (dT) and Moloney murine leukaemia virus reverse transcriptase (M-MLV RT; Promega®), adapted from the manufacturers protocol. And before the synthesis treated with RQ1 RNase Free DNase (Promega ®).

All the qPCR test, validations and experimental steps followed the Applied Biosystems (Thermo Scientific TM) recommendations. All the qPCR analysis were performed in the BioRad CFX96 *Touch Real-Time PCR Detection System* (BioRad) using specific designed primers sequenced (Supplmentary Table) for the genes *VuGOX1(Vigun01g052400)*, *VuGOX2(Vigun03g162000)*,*VuGOX3(VigunL052501)*, *VuCATa (Vigun09g260100), VuCATb (Vigun08g001400), VuCATc (Vigun05g264800),* and CPSMV-CP. Genomic and CDS (coding sequences) were retriever from the Phytozome v13 (https://phytozome-next.jgi.doe.gov) and the CPSMV-CP from the NCBI (National Center for Biotechnology Information) data bases (https://www.ncbi.nlm.nih.gov) (Supplementery Table 1). Amplification reactions were performed as the following steps: 95 °C for 10 min, 40 circles of 94 °C for 15 s and 62 °C for 1 min, and the disassociation step of 95 °C for 1 s. The relative expression of the target genes was performed as described by Pffafl (2001), and the endogenous reference *VuUBQ3*() was used (Supplementary Table 1).

3.2.8 Virus detection

All cowpea plants mock and infected were maintained at green house condition until the presence of clear symptoms (Supplementary Figure 1).

3.2.9 Identification of catalase *cis*-elements in *V. unguiculata*

For the *cis*-elements identification 1500 bp sequence upstream of the start codon of CAT genes were retrieved from the Phythozome v13 (https://phytozome-next.jgi.doe.gov) and used for the analysis.

3.2.10 Database search, sequence retrieval, and analysis of physical properties of CAT protein members

The subcellular localization of VuCAT and VuGOX proteins was predicted using CELLO 2.5v: sub-cellular localization predictor (CELLO:Subcellular Localization Predictive System) and WoLF pSORT prediction software (WoLF PSORT: Protein Subcellular Localization Prediction Tool) (Supplementary Table 3; Supplementary Figure 2). For the estimated protein molecular weight (MW) and isoelectric point (pI), the Expasy tool (https://web.expasy.org/compute_pi/) from the SIB (Swiss Institute of Bioinfomatics) was used (Bjellqvist et al., 1993; Biellqvist et al., 1994; Gesteir et al., 2005). All aminoacids (aa) sequences were retrieved from the Phytozome v13 database, and the confirmation of functional domain from VuCAT was performed using the InterPro 106.0 tool (https://www.ebi.ac.uk/interpro/) from the EMBL's European Bioinformatics Institute. All VuGOX protein sequences were selected based on the work of Roque et al. (2023).

3.2.11 Identification of catalase *cis*-elements in *V. unguiculata*

For the *cis*-elements identification, 1500 bp sequences upstream of the start codon of CAT and GOX genes were retrieved from the Phytozome v13 (https://phytozome-next.jgi.doe.gov), as previously described, and was used for the analysis (Roque et al., 2023).

3.2.12 Phylogenetic tree construction

Phylogenetic relationships were reconstructed by multiple sequence alignment of CDS from *Arabidopsis thaliana* (AT1G20630.1, AT4G35090.3, and AT1G20620.6), *Oryza sativa* (Os02g02400.1, Os06g51150.1, Os03g03910.1, and Os04g39780.1), *Glycine max* (Glyma.04G017500.1, Glyma.06G017900.1, Glyma.14G223500.1, and Glyma.17G261700.1), *Sorghum bicolor* (Sobic.001G517700.1, Sobic.010G274500.2,. and Sobic.004G011566.2), *Chlamydomonas reinhardtii* (Cre01.g045700.t1.1 and Cre09.g417150.t1.2). For *V. unguiculata* entries were used previously CDS commented. For the multiple alignment performance, the MUSCLE tool of the MEGA12 software was used (https://www.megasoftware.net; Kumar et al., 2018). For topology reconstruction validation., Neighbour-Joining analysis was performed, using a bootstrap of 1000 replications.

3.2.13 Statistical Analyses

The experiments were arranged in an entirely randomized design, and all analysis were carried out using five independent biological replicates. Data from physiological, biochemical, and relative expression assays were compared using One-Way analysis of variance (ANOVA) followed by Tukey's statistical parametric variance test ($p \leq 0.05$) for comparison between the means of the treatments.

3.3 RESULTS

3.3.1 Phenotypic traits of *V. unguiculata* cultivars post CPSMV inoculation and oxidative damage parameters

Secondary leaves from the third trifoliate leaf of each treatment does not manifest any symptoms in both cultivars at all collection times (Figure 1 a-l). However, after 14 days of CPSMV inoculation, Pitiúba plants, reported as susceptible to the virus, demonstrate symptoms of mosaic in younger leaves, characteristic of CPSMV (Supplementary Figure 1.).

Hydrogen peroxide accumulation in leaves tissue was evaluated in secondary leaves from the infected trifoliolate by DAB staining, however, due to the early stages of infection no characteristic HR points were observed (Figure. 1 a-l), only some stains from pigmentation and H_2O_2 from the tissue.

Besides the hydrogen peroxide content, malonadialdehyde content was also quantified in secondary leaves after CPSMV infection. Lipid peroxide content was observed increased only in Pitiúba plants infected in both 16 (Figure 1m) and 48h times (Figure 1n). As a contrast the MDA content, an indicative of lipid peroxidation, in the Macaibo resistant cultivar no increase was observed in both treatments (Figure 1 n-o).

3.3.2 Catalase activity were lower at early hours at the susceptible cultivar under CPSMV infection

Catalase activity was measured in all three times after CPSMV inoculation, however only at the 16 hours post inoculation was observed significant difference among treatments and cultivars (Figure 2a). Where the Mo16-P was noticed lower when compare with the same genotype infected with CPSMV, however, the Mo16-M shown an increased activity when comparing mocking plants, and no difference in the activity

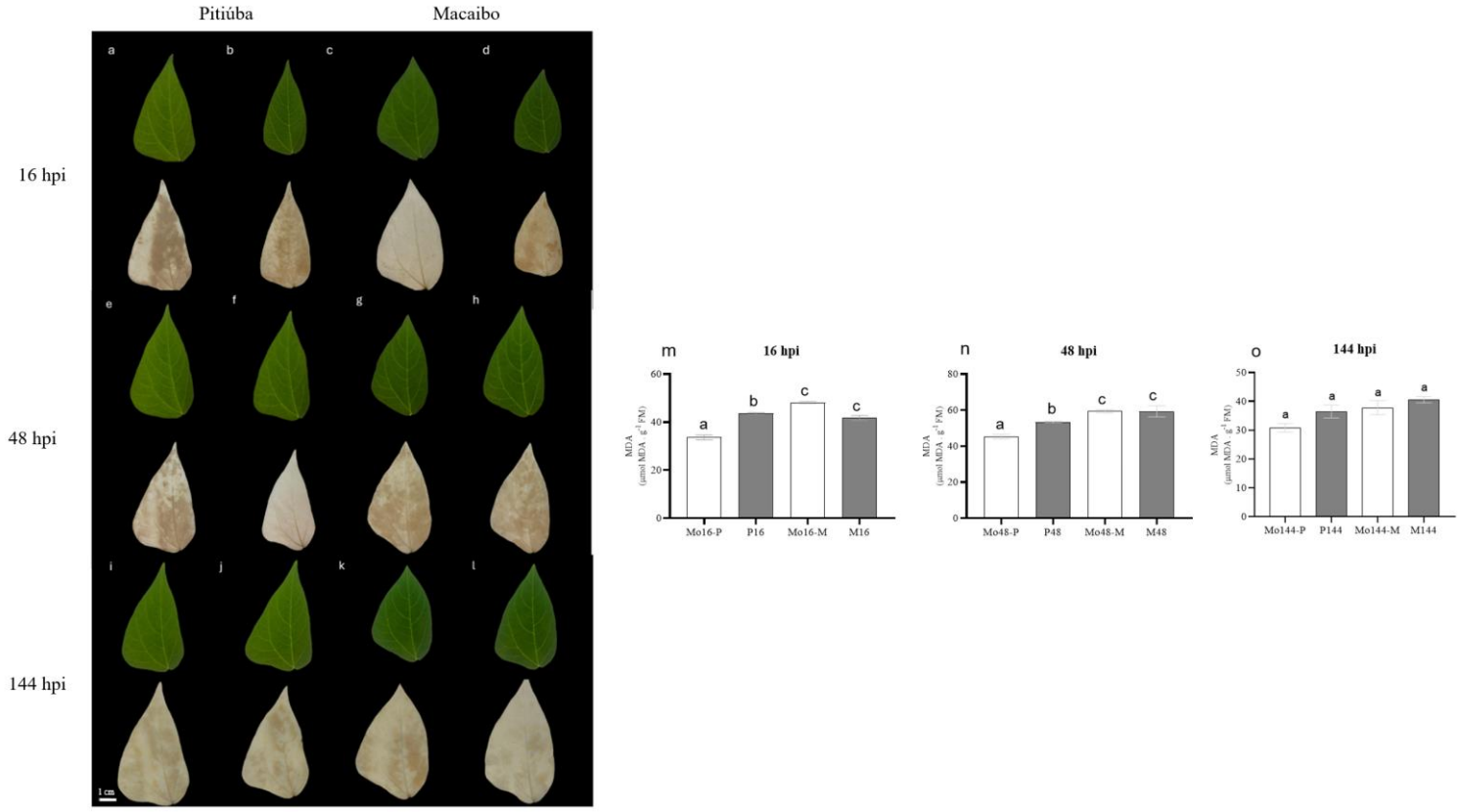

Figure 1. *Vigna unguiculata* secondary leaves from Macaibo (M) and Pitiúba (P) cultivars, collected and treated to observe the H_2O_2 accumulation after 16, 48 and 144 hours post inoculation (hpi) and mock (Mo). And malondialdehyde (MDA) content of infected leaves. Leaves were stained with 3,3'-diaminobenzidine (DAB). Different lowercase letters indicate significant differences among treatments according to Tukey's significance test ($p \leq 0.05$). Columns indicate means of four biological replicates and bars indicate standard error deviation (±).

in infected plants (M-16). And the activity of Pitiúba increasing with 48 and 144 hours in the mock condition.

To reinforce and confirm the data from DAB staining and CAT activity from both cultivars under all three infection conditions, hydrogen peroxide was measured in the secondary leaves from the infected trifoliate. At 16 hours post inoculation the content of H_2O_2 was equal among untreated leaves and infected ones (Figure 2d), however was possible to perceive a difference between both cultivars, where in both conditions (Mock and infected) the Macaibo cultivar demonstrated a lower hydrogen peroxide content on its leaf, where the susceptible shown higher levels. The same pattern was observed in both cultivars after 48 hpi, indicating no changes in the H_2O_2 levels after the infection on secondary leaves (Figure 2e).

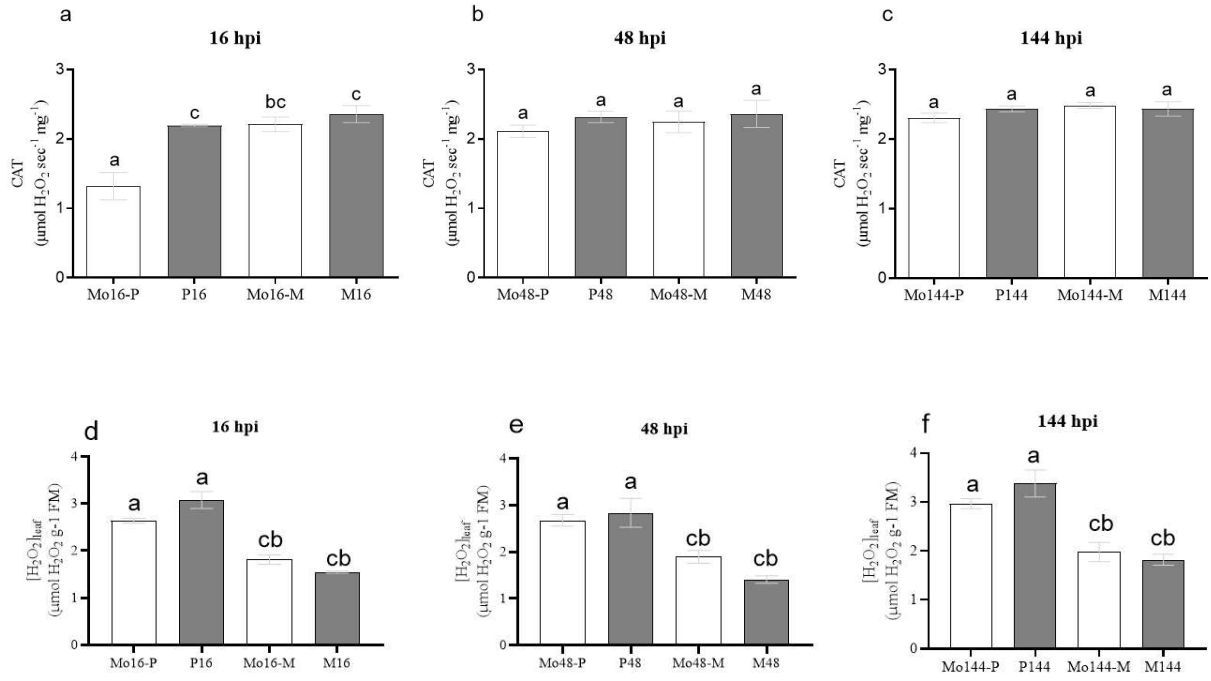

Figure 2. Catalase activity profile and hydrogen peroxide (H_2O_2) content in *V. unguiculata* leaves in non-inoculated and inoculated after 16, 48, and 144 hours post inoculation (hpi). Different lowercase letters indicate significant differences among treatments according to Tukey's significance test ($p \leq 0.05$). Columns indicate means of four biological replicates and bars indicate standard error deviation (±).

3.3.3 Quantitative PCR of *V. unguiculata* GOX and CAT genes and *cis elements* identification

Aiming to understand the correlation between the different hydrogen content among both cultivars, but with similar catalase activity, quantitative PCR (qPCR) analysis was performed to evaluate the expression from the different gene copies from both glycolate oxidase and catalase, due to its role in the H_2O_2 balance (Figure 3).

Among all the transcript analysed, it was perceived an expression change in the *VuGOX1* gene only in the Macaibo cultivar 16 hours post inoculation, where in Mock plants the expression levels were downregulated (Figure 3a), and the expression levels of *VuGOX1* among the cultivars demonstrates different expression levels. *VuGOX1* expression levels were not statistically significant between the two cultivars when comparing Mock and infected after 48 hours post inoculation (Figure 3b). The *VuGOX1* expression was not s The *VuGOX2* gene, which is the most expressed among the genes and cultivars, does not shown any differential levels of expression among Mock and inoculated plants, in both 16hpi and 48hpi (Figure 3a-b). However, the levels of transcripts of *VuGOX2* in Macaibo cultivar were lower when compared with Pitiuba at 16hpi, raising after 48hpi (Figure 3a-b).

The *VuCATc* expression levels followed a profile similar to the other genes previously mentioned, with no significant differences between Mock and infected plants at 16 hpi, only among the cultivar's differences were perceived, where the *VuCATc* levels in Macaibo were lower (Figure 3a). However, at 48hpi the levels of *VuCATc* in the Pitiuba infected plants were shown upregulated, when compared with Mock plants, and Macaibo plants shown not statistically significant between treatments (Figure 3b). *VuGOX3* and *VuCATa* no reads were detected.

To correlate the levels of expression with the CPSMV stimuli, *cis-elements* from promoter regions of GOX and CAT from cowpea were analysed, where in the total 36 types promoters were identified among all genes evaluated, excluding those related only to transcriptional process and light response. Among all the promoters identified the abscisic acid responsive element (ABRE; ABRE3a; ABRE4), light responsive element (3-AF3 binding site), elements associated to MYB transcription factor (MYB; MYB recognition site; MYB-like sequence), cis-acting regulatory element essential for the anaerobic induction (ARE), cis-acting regulatory element related to meristem expression (CAT-box), MYBHv1 binding site (CCAAT-box), cis-acting regulatory element involved in the MeJA-responsiveness (CGTCA-motif; TGACG-motif), dehydration-

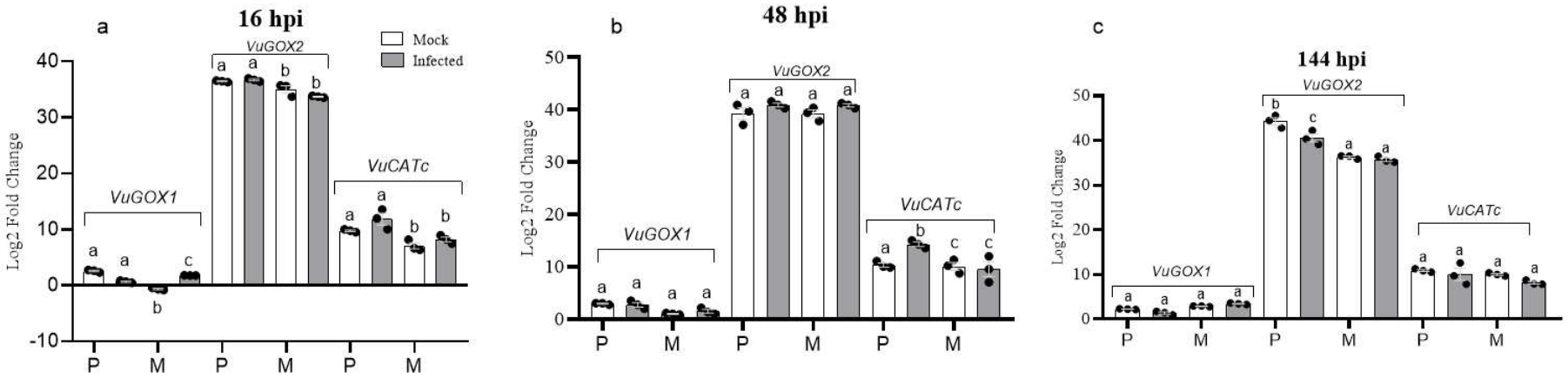

Figure 3. Relative expression profiles of Glycolate Oxidase (GOX) genes, *VuGOX1* and *VuGOX2*, and Catalase (CAT), *VuCATc*, from leaves collected after Cowpea Severe Mosaic Virus infection times of 16, 48, and 144 hours post inoculation (hpi). Gene expression was normalized using as reference gene *VuUBQ3*. Different lowercase letters indicate significant differences among treatments according to Tukey's significance test ($p \leq 0.05$). Columns indicate means of three biological replicates and bars indicate standard deviation (±).

responsive element (DRE-1), ethylene-responsive element (ERE), hormone-responsive element (F-box) and gibberellin-responsive element (GARE-motif) were reported (Supplementary Table 1.).Also, the cis-acting element involved in low-temperature responsiveness (LTR), MYB binding site involved in drought- inducibility (MBS), MYB binding site involved in flavonoid biosynthetic genes regulation (MBSI), MYB binding site involved in light responsiveness (MRE), abiotic stresse-responsive element (MYC) and gibberellin-responsive element (P-box; TATC-box).

The cis-element involved in salicylic acid responsiveness (TCA; TCA-element), cis-acting element involved in defense and stress responsiveness (TC-rich repeats), auxin-responsive element (TGA-element), stress-responsive element (STRE), cis-acting regulatory element involved in high temperature (WRE3), and wound responsive element (WUN-motif) was also identified. All the other *cis-elements* not cited has not known function, such as AAGAA-motif, ACTCATCCT sequence, AP1, as-1 and box S.

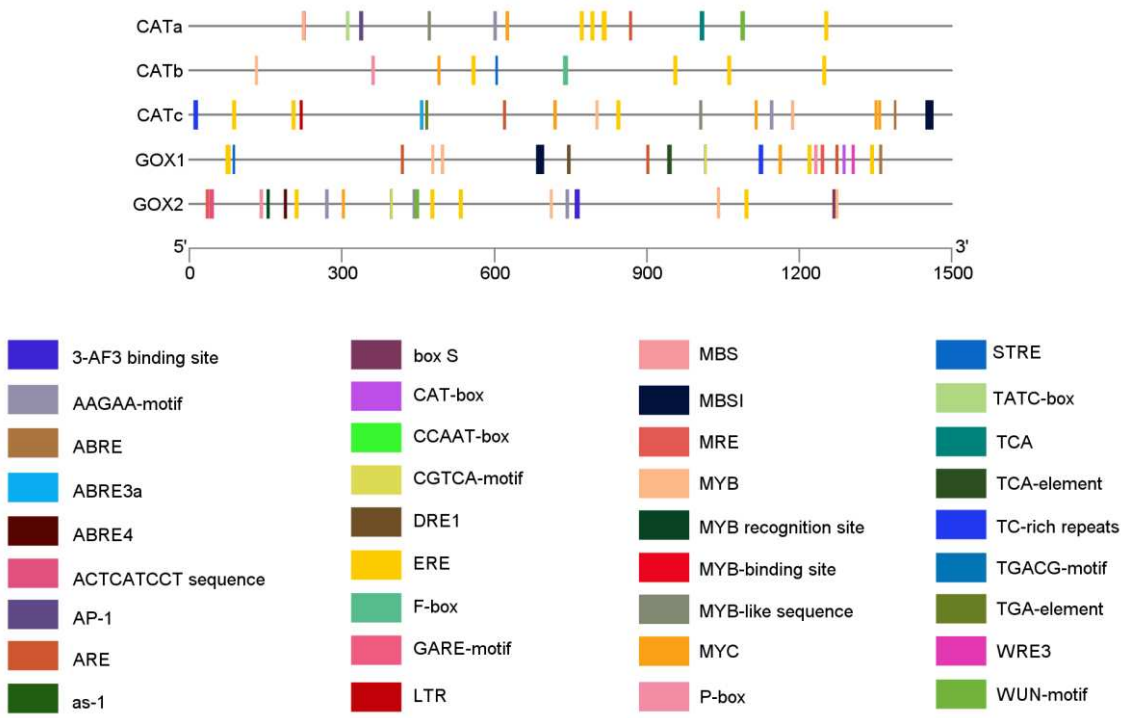

Figure 4. Cis-*elements* from promoter region of Glycolate Oxidase (GOX) and catalase (CAT) genes from *Vigna unguiculata*. Coloured blocks indicate distinct *cis-elements* present in the promoter region.

Also, physical properties of *VuCAT* and *VuGOX* were analysed, where the conservated domain of Catalase, the heme-binding pocket (cd08154) was observed in

both VuCATa and VuCATb (Table 1). The *V. unguiculata* catalase gene copies were present in two different chromosomes, chromosome eight for VuCATa and chromosome nine for VuCATb, and the transcripts coding only for one protein each (Table1). Also, protein polypeptide, CDS sequence, isoelectric point, and molecular weight among catalases were remarkably similar, and both predicted sub-cellular localization for the peroxisome organelle as expected (Table 1).

Table 1. List with detailed information about Catalase and Glycolate Oxidase in *Vigna unguiculata* along with their gene and protein identification/alternative splicing forms, chromosome location, coding sequences, polypeptide length, and predicted molecular weight, isoelectric point (pI), and subcellular localization.

Gene	Protein	Locus name	CDS(bp)	Protein(aa)	MW(kDa)	pI	Localization
VuCATa	VuCATa.1	Vigun08g001400.1	1479	493	57.06243	6.56	Peroxisome[a,b]
VuCATb	VuCATb.1	Vigun09g260100.1	1479	493	56. 781	6.8	Peroxisome[a,b]
VuGOX1	VuGOX1.1						
	VuGOX1.2	Vigun01g052400	1119	373	40.92529	9.02	Peroxisome[a,b]
	VuGOX1.3						
VuGOX2	VuGOX2.1						
	VuGOX2.2						
	VuGOX2.3	Vigun03g162000	1107	369	40.34485	9.16	Peroxisome[a,b]
	VuGOX2.4						
	VuGOX2.5						
	VuGOX2.6						
VuGOX3	VuGOX3.1	VigunL052501	1158	386	41.90391	9.98	Mit[a]; Cyt[b]

Abbreviations: CDS, coding DNA sequences; aa, aminoacids; MW, molecular weight; pI, isoelectric point; Mit, mitochondria.

[a] CELLO v.2.5: sub-cellular localization predictor (CELLO:Subcellular Localization Predictive System);

[b] WoLF pSORT prediction software (WoLF PSORT: Protein Subcellular Localization Prediction Tool).

Glycolate oxidase physical properties was also analysed, where all the copies share similar traits, such as CDS and protein length, molecular weight, and pI. However, the number of coding protein was very variable, with *VuGOX1* gene resulting in three different proteins, and *VuGOX2* coding for six proteins, both from different chromosomes, one and three, respectively, and with similar sub-cellular localization, in the peroxisome (Table 1). And more distinguish was the *VuGOX3* gene, which was observed previously in a contig, having similar traits to other GOX members, however coding only one protein, and having as it is sub-cellular localization the Mitochondria, something already observed in other species, such as *A. thaliana* (Table 1).

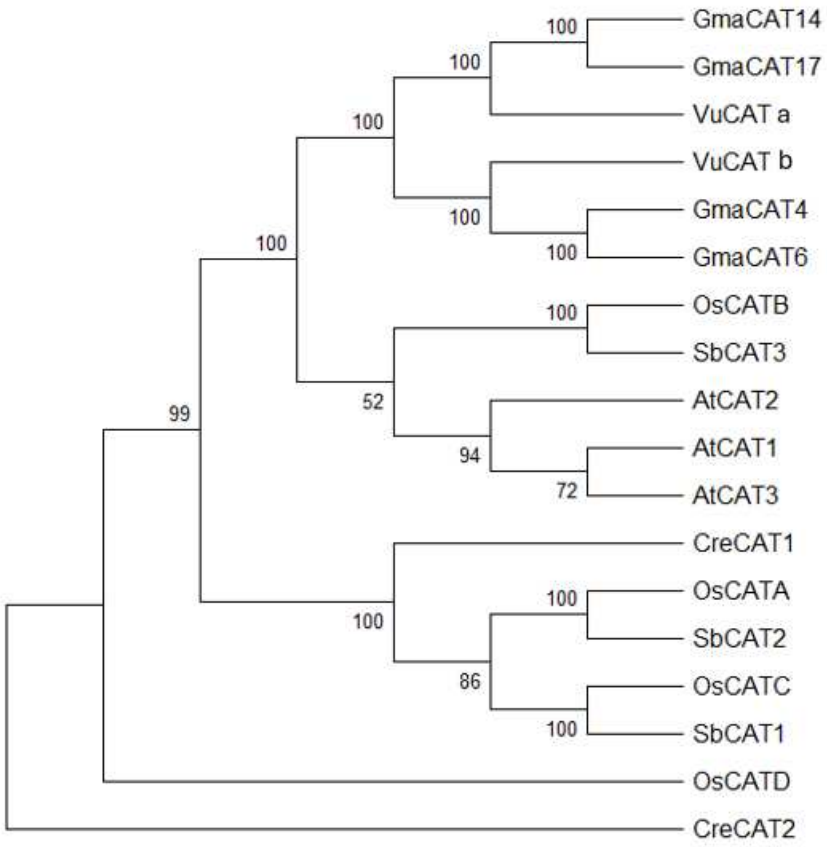

Figure 4. Phylogenetic relationship among Catalase orthologs in model and *V. unguiculata* plants. All sequences of Catalase coding DNA sequence were retrieved from the Phytozome database. With a rooted phylogenetic tree constructed based on the Neighbour-Joining method from the software MEGA 12 tool using a bootstrap of 1000 replications. Where the abbreviations from each species being Gma, *Glycine max*, Vu,

Vigna unguiculata, Os, *Oryza sativa*, Sb, *Sorghum bicolor*, At, *Arabidopsis thaliana*, and for Cre, *Chlamydomonas reinhardtii*. Each sequence identification are presented in the Material and Methods section.

A phylogenetic tree was constructed to observe the evolutionary relationship among *VuCAT* genes and other plant models more and less related through the evolution course, such as *G. max*, *S. bicolor*, *O. sativa*, and *A. thaliana*(Figure 4).

3.4 DISCUSSION

3.4.1 Lipid peroxidation indicates damage from CPSMV inoculation

The presence of symptoms in the susceptible cultivar was expected due to the compatible interaction already reported between the Pitiúba and CPSMV (Booker et al., 2007; Mandadi; Scholthof, 2013; Souza et al., 2017; Souza et al., 2020). Which was confirmed after 2 weeks post inoculation (Supplementary Figure 1a.), with only Macaíbo and Mock plants remained asymptomatic (Supplementary Figure 1b-d). Where plants from both cultivars at 16, 48, and 144 post inoculation, shown no clear symptoms characteristic of the CPSMV, as expected (Figure 1a-l)

As a form to evaluate the initial infection and how both contrasting cultivars would response to CPSMV infection and its relationship with oxidative burst the DAB staining was used, as method to detected hydrogen peroxide accumulation in leaves tissues at early hours post inoculation (Souza et al., 2020). Due to the role of ROS molecules, manly the H_2O_2, as a key molecule to act as a signal in the early stages of pathogen response, due to its stability and permeability (Costa *et al*, 2010; Neill et al., 2002; Mittler et al., 2011; Cui *et al*., 2016). Previous works from Varela and coworkers (2017) using gel-free/label free analysis of cowpea plants infected with CPSMV demonstrated the increase of peroxisomal (*S*)-2-hydroxy-acid oxidase (GLO), related to the hydrogen peroxide production, which lead to H_2O_2 elevating content, in plants infected after 2 and 6 days, possible related to CPSMV response (Rojas et al., 2012). However, no significant phenotype alteration was observed among the cultivars in distinct collection times, with no presence of previous characteristic symptoms described, only with secondary leaves presenting brownish stains prevenient from residual pigments and H_2O_2 normal content from the tissue (Figure 1 a-l).

However, as commented ROS production and it role as a signal molecule by the plant is followed by a great risk, giving the fact the high concentration of reactive species could lead to peroxidation of membrane lipids, which are toxic to cells that can cause great damage to vegetal cell and even, in the last stage, cell death (Wu et al., 2006; Sharma et al., 2012). The malondialdehyde content in secondary leaves were evaluated, and only in the susceptible cultivar (Pitiúba) the lipidic oxidated content were higher when compared with the Mock plant, in both 16 and 48 hpi (Figure 1 m-n). Indicating that in Macaíbo plants is possible to be present a mechanism related effective ROS mitigation, probable through an antioxidative enzymes apparatus, thus not being harmful to leaf tissues, while the susceptible cultivar had an increase in the lipidic peroxidation levels (Varela et al., 2017). Thus, due to the importance of hydrogen peroxide importance and catalase role in the H_2O_2 homeostasis, CAT total activity and H_2O_2 content was investigated.

3.4.2 Hydrogen peroxide content was different among the genotypes

Among the antioxidant enzymes related with the hydrogen peroxide and its relationship with pathogen response, the Catalase enzymes are responsible to scavenge H_2O_2, manly in the peroxisome, and turn this ROS in water and oxygen (Nicholls et al., 2000; Zhang et al., 2016; Riseh; Fathi; Vatankhak; Kennedy, 2024). Thus, among all the treatments only Mo16-P shown a reduced activity of catalase when compared with P-16 (Figure 2a), probably related to the infection or damage caused by the CPSMV inoculation, acting as a mechanism to mitigate the upcoming ROS stress.

In contrast, Macaíbo at the same conditions, had a similar catalase activity among both treatments (Figure 2a). With this difference not observed in plants Mock and inoculated collected after 48 and 144 hours post inoculation in both cultivars (Figure 2 b-c). This higher activity of catalase at early hours of inoculation observed in Macaibo plants, in parallel with Pitiúba, can indicate a mechanism related to CPSMV resistance altogether with the lower levels of lipid peroxidation. Giving the fact that H_2O_2 content at Macaibo cultivar, could be observed a stable content among treatments (Figure 2 d-f).

Where the lower content of H_2O_2 in Macaíbo secondary leaves after the CPSMV infection could indicate to us a mechanism not related to an oxidative burst at first, due to a lower and stable concentration of hydrogen peroxide and low catalase enzyme

activity hours post inoculation. Where the balance of ROS, more specifically hydrogen peroxide, being controlled local and systematically in plants reported by Li et al. (2023) by Ca^{+2} accumulation in the cytosol, which leads to the association of Glycolate Oxidase – Catalase (GOX-CAT) Switch complex, responsible to control the intracellular hydrogen peroxide balance, leading to a decrease of the ROS content (Zhang et a., 2016).

However, in the susceptible cultivar, the opposite could be observed, with a higher level of hydrogen peroxide, combined with a lower activity of CAT enzyme, probably indicating a disassociation of the GOX-CAT Switch complex. Where an increase of ROS, after the plant cell recognize of damage molecular patterns (DAMPs) or even pathogen effectors, such as ssRNA from the CPSMV, through compatible interaction lead the cell plant to early pattern immunity trigger (PTI) and with the infection persistence, the effector immunity trigger (ETI), the cell organism maintained the reactive species burst, leading to cell death, also reinforced by lipid peroxidation content (Janes and Dangl, 2006; Katagiri and Tsuda, 2010; Dangl et al., 2013; Jones et al., 2024).

Nevertheless, due to importance of the GOX-CAT switch complex and it is possible role in the CPSMV immunity, it was of our interest to understand the expression pattern at systemic infection level of GOX and CAT transcripts.

3.4.3 *VuGOX* and *VuCAT* transcripts were modulated after the inoculation with CPSMV

A previous work of our team performed a. Genome-wide analysis in cowpea plants identified three genes of GOX in its genome, *VuGOX1* (*Vigun01g052400*), *VuGOX2* (*Vigun03g162000*) and V*uGOX3* (*VigunL052501*), and were named as so due to its similarity of *Arabidopsis thaliana* copies (Roque et al., 2023). And here we recognized two genes of Catalase in cowpea genome, being *VuCATa* (*Vigun09g260100*), *VuCATb* (*Vigun08g001400*), where *VuCATa* and *VuCATb* being more similar to *AtCAT1* and *AtCAT2*, respectively (Table 1; Supplementary 3).Also, sub-cellular localization prediction of both catalase protein pointed to the *peroxisome* organelle, similar to the VuGOX1 and VuGOX2 proteins, reinforcing they play in the GOX-CAT switch and hydrogen peroxide balance in *V. unguiculata*. However, interestingly the VuGOX3 protein shown as predicted sub-cellular localization the mitochondria, similar to *A.*

thaliana AT3 protein, involved in the L-lactate metabolism (Roque et al., 2023; Engqvist et al., 2015)

Here, we observed that the transcript levels of *VuGOX1* were only differential in Macaibo plants in infected plants at the early hours after inoculation, possible being related to hydrogen peroxide production as a signal molecule to systematic acquire resistance of CPSMV (Figure 3a), where no Pitiúba expression profile was observed altered. This could indicate in Macaibo a upregulation of *VuGOX1* to act in plant defence mechanism due to CPSMV infection, which are maintained at 48 and 144 hpi (Figure 3 b-c). In the Pitiúba cultivar the *VuGOX1* expression pattern was not altered in all times analysed (Figure 3 a-c). Thus, this absence of alteration in the expression profile of GOX is probably related to the incapability of Pitiúba genotype to respond to the CPSMV infection, where previous works using mutated plants from the same cultivar which present a resistance phenotype, shown an increase of abundance of GOX proteins after 7 of infection (Souza et al., 2020).

VuGOX2 gene does not demonstrate differential expression among treatment at 16 hpi, however the expression levels among cultivar were distinct, with a slightly reduction of the transcription in the Macaíbo cultivar (Figure 3a). With the expression profile been similar among cultivar and treatments after 48 hours of inoculation and reducing again the transcription levels after 144 hpi for all Macaíbo treatments and infected Pitiúba (Figure 3 b-c). These data which could corroborated the previous observations with *VuGOX1*, however the GOX transcripts levels of Macaíbo only increasing after 48 hpi, being similar to Pitiúba expression, and decreasing againd after 144 hpi (Figure 3 b-c). And 144 hpi the levels of *VuGOX2* in inoculated Pitiúba plants were downregulated in comparison to Mock (Figure 3c).

And *VuCATb* demonstrated differential among cultivars, where 16 hpi treatments have a similar profile with Mock plants, and Pitiúba having higher levels of expression tha Macaíbo (Figure 3a). However, after 48 hours post inoculation the transcript levels of *VuCATb* in infected Pitiúba plants were higher than Mock and Macaíbo plants, probably related to the oxidative burst in response to the pathogen infection. And all expression profiles being similar after 144 hpi. Where that increase of catalase transcripts are related to the higher activity in infected Pitiúbas plants at 16hpi

and 48hpi, which are similar in 144 hpi (Figure 2), which for viruses can help the disease establishment already reported in other plants (Mathioudakis et al., 2013).

Thus, our data suggest that GLO and CAT must have a crucial role in CPSMV response and resistance mechanism. As was previous seen in works model plants such as *Nicotiana benthamiana* where viral particle from the BSMV (Barley Stripe Virus) interacts with the GOX protein, inhibiting glycolate oxidase activity, which leads to a lower production of ROS in the early stages of infection thus allowing infection to occur (Yang et al., 2017). Thus, we evaluate the *Cis*-elements from promoter regions from all *VuGOX* and *VuCAT* that we identified in the cowpea genome, as a form to correlate with the expression profiled shown and it is relation with CPSMV infection.

3.4.4 *Cis-elements* from promoter regions from all *VuGOX* and *VuCAT* can shed a light in how the cowpea cultivars respond and modulate the expression levels

Thus, due to the information obtained by gene expression of *VuGOX1, VuGOX2* and *VuCATb* after inoculation with CPSMV, *cis-elements* from all *VuGOX* and *VuCAT* copies from *V. unguiculata* were analysed as a form to relate the differential expression and the present promoters (Figure 3d). Among the interesting *cis-elements* the ones which are involved in salicylic acid responsiveness (TCA; TCA-element), cis-acting element involved in defense and stress responsiveness (TC-rich repeats), auxin-responsive element (TGA-element), stress-responsive element (STRE), cis-acting regulatory element involved in high temperature (WRE3), and wound responsive element (WUN-motif) (Figure 4). Still, a great part of the *cis-elements* detected are related to stress conditions, more specifically abiotic, such as MYB, cis-acting regulatory element essential for the anaerobic induction (ARE), MYB binding site involved in drought-inducibility (MBS), abiotic stresse-responsive element (MYC), MYBHv1 binding site (CCAAT-box), dehydration-responsive element (DRE-1) and ethylene-responsive element (ERE) (Fujimoto et al., 2000; Narusaka et al., 2003; Li; Mizoi et al., 2013; Ng; Fan, 2015; Kaur et al., 2017; Kang et al., 2022; Lazar et al., 2014;). Also, the WUN-motif, which is related to biotic stress, the wound responsive element (ain-Ali et al., 2021).

An important *cis*-element observed was the TCA-element, which is related to salicylic acid response and pathogen defences, and could participate in the dynamic between GOX-CAT switch complex association-dissociation dynamic, which was

proposed to be regulated by SA signalling, modulating hydrogen peroxide waves, important to abiotic and biotic stimuli (Raskin, 1992; Zhang et al., 2016), and having a possible relation with the resistance mechanism (Kamle et al., 2020).

And phylogenetic tree analysis grouped the *VuCAT* conding DNA sequences with catalase sequences from *G. max* (Figure 4), which are related to drought stress and heat stress, and upregulated in plant organs such as young leaves, flower tissues, root and nodule, with same predicted sub-cellular localization (Aleem et al., 2022).

Thus, incompatible interaction, such as reported in Macaibo, is supposed to occurs where the plant recognizes viral elicitors and rapidly response through signal cascades, such as oxidative burst, with the production of oxygen reactive species, hypersensitive response (HR), accumulation of pathogen-related proteins (PR-proteins) and systematic acquired resistance (SAR), and not showing the classic pathogen symptoms (Camarço et al., 2009; Mandadi; Scholthof, 2013). Other type of mechanism of tolerance of CPSMV infection already reported in cowpea plants is the RNA silencing through micro RNA (miRNA), leading to the synthesis of double strand RNA (dsRNA), which are processed by Dicer-lie proteins (Dicer RNase), generating small RNAs (sRNAs) which will lead to the formation of the Argonaute and RNA-induced silencing (AGO-RISC) complex(Martins et al., 2020). Where Macaíbo plants could act through the AGO-RISC complex leading to resistance and the ROS regulation, mediated by the GO-CAT complex responsible to the systemic acquired resistance to other plant tissues (Figure 4). While the Pitiúba plants, which could be not capable to recognize early the pathogen effectors, are led to ETI pathway resulting in the ROS burst, lipid peroxidation, HR, and cell death as a tentative to restring CPSMV virus systemic proliferation (Figure 4).

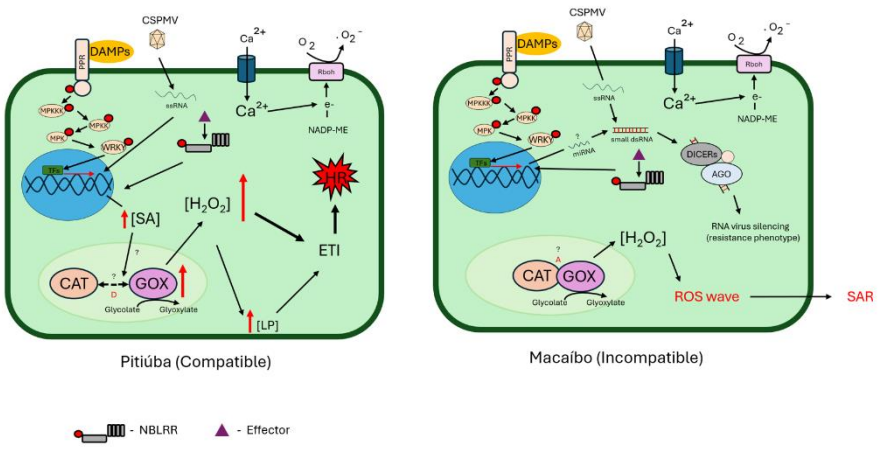

Figure 4. Overview of possible pathway that could be acting in both Pitiúba (susceptible) cultivar, which presents a compatible interaction with CPSMV virus, and Macaíbo (resistant), reported with an incompatible interaction with the CPSMV virus. Abbreviations: SA, salicylic acid; GOX, glycolate oxidase; CAT, catalase; ROS, reactive oxygen species; H_2O_2, hydrogen peroxide; SAR, systematic acquired resistance, HR, hypersensitive response; ETI, effector trigger immunity; PTI, pattern trigger immunity; NBLRR, nucleotide; Rboh, NADPH oxidases; ssRNA, single strand RNA; DAMPs; damage-associated molecular pattern; NLR, nucleotide-binding leucine-rich-repeat receptor; LP, lipid peroxidation; TFs, transcription factors; PRR, pattern recognition receptors.

Other crucial point, beside the previous one commented, is the capability of the vegetal organism during the pathogen infection, such as virus, to provide energy from the primary metabolism support cellular requirements for plants defence response and could cause symptoms to manifest much later than compared with new leaves (Bolton, 2009; Kangasjarvi et al., 2012; Rojas et al., 2014), which could give us a hint about the differences of enzymatic, transcriptional and biochemical patterns observed in the present work and the mild/delayed symptoms shown in the Pitiúba genotype. Considering that previous works already brought the importance of photosynthesis and photorespiration apparatus to plant resistance (Souza et al., 2020; Souza and Carvalho, 2019).

3.5 CONCLUSION

Thus, our present work compared two contrasting cowpea genotypes inoculated with CPSMV after 16 and 144 hours post inoculation, aiming to understand the aspects behind the resistance phenom. Our finding supported past studies using younger plants that the redox apparatus seems to play a key role in response to CPSMV infection, and later resistance. Where the transcription of GOX in the first few hours after virus inoculation together with a higher activity of catalase seem to be correlated with the process of acquired systemic resistance, this for the resistant genotype. While susceptible plants showed no modulation at the transcript level of the GOX enzyme, they did show a higher level of hydrogen peroxide and peroxidised lipids, indicating processes related to the HR and ETI phenomenon. Thus, through biochemical, molecular and bioinformatics data, our work suggests that the GOX-CAT switch complex acts during the response to the pathogen, modulating its response locally and systemically.

Contributions

We declare all the following authors contributed to the present work, and agree with the manuscript in its current form:

1 – Victor Breno Faustino Bezerra (VBFB) – Author;

3 – João Victor Dourado Alves Brito (JVDAB);

4 – Gabriela Oliveira Matos (GOM);

5 – Lorenna Maria Neves Freitas (LMNF);

6 - Murilo Siqueira Alves (MSA) – corresponding author.

MSA and VBFB: Conceptualization; MSA: Project administration; VBFB, JVDAB, GOM, MSA: Investigation and Methodology; MSA: Supervision; VBFB and MSA: Validation; VBFB: Writing - original draft; VBFB and MSA: Writing - review and editing; MSA: Visualization.

Statements and Declarations

Authors declare they don't have competing interests related to the work submitted for publication.

Acknowledgements

We thank the Conselho Nacional de Desenvolvimento Científico e Tecnológico (CNPq; grant number 423471/2018-0) and Coordenação de Aperfeiçoamento de Pessoal de Nível Superior (CAPES) who supported this study.

REFERENCES

AIN-ALI, Qurat-Ul; MUSHTAQ, Nida; AMIR, Rabia; GUL, Alvina; TAHIR, Muhammad; MUNIR, Faiza. Genome-wide promoter analysis, homology modeling and protein interaction network of Dehydration Responsive Element Binding (DREB) gene family in Solanum tuberosum. **Plos One**, [S.L.], v. 16, n. 12, p. e0261215, 16 dez. 2021. Public Library of Science (PLoS). http://dx.doi.org/10.1371/journal.pone.0261215.

ALEEM, Muqadas; ALEEM, Saba; SHARIF, Iram; ALEEM, Maida; SHAHZAD, Rahil; KHAN, Muhammad Imran; BATOOL, Amina; SARWAR, Gulam; FAROOQ, Jehanzeb; IQBAL, Azeem. Correction: aleem et al. whole-genome identification of apx and cat gene families in cultivated and wild soybeans and their regulatory function in plant development and stress response. antioxidants 2022, 11, 1626. **Antioxidants**, [S.L.], v. 14, n. 2, p. 229, 18 fev. 2025. MDPI AG. http://dx.doi.org/10.3390/antiox14020229.

AVERYANOV, A. Oxidative burst and plant disease resistance. **Frontiers in Bioscience - Elite**, v. 1 E, n. 1, p. 142–152, 2009.

BACETE, Laura; MÉLIDA, Hugo; MIEDES, Eva; MOLINA, Antonio. Plant cell wall-mediated immunity: cell wall changes trigger disease resistance responses. **The Plant Journal**, [S.L.], v. 93, n. 4, p. 614-636, fev. 2018. Wiley. http://dx.doi.org/10.1111/tpj.13807.

BASTOS, E. A. et al. **A cultura do feijão-caupi no Brasil**. [s.l: s.n.]. v. 1p. 1–71. Disponível em: https://www.google.com/url?sa=t&rct=j&q=&esrc=s&source=web&cd=&cad=rja&uact=8&ved=2ahUKEwjTpIvkqaTAxVhqpUCHe0WGzgQFnoECB4QAQ&url=https%3A%2F%2Fwww.infoteca.cnptia.embrapa.br%2Finfoteca%2Fbitstream%2Fdoc%2F6060%2F1%2FCulturaFeijaoCaupi.pdf&usg=AOvVaw3vFmgVioDMGLVPlLXFX_&opi=89978449. Acesso em: 23 de jan. de 2025.

BEERS, R. F.; SIZER, I. W. A spectrophotometric method for measuring the breakdown of hydrogen peroxide by catalase. **Journal of Biological Chemistry**, v. 195, p. 133–140, 1952. Acesso em: 23 de jan. de 2025.

BJELLQVIST, Bengt; BASSE, Bodil; OLSEN, Eydfinnur; CELIS, Julio E.. Reference points for comparisons of two-dimensional maps of proteins from different human cell types defined in a pH scale where isoelectric points correlate with polypeptide

compositions. **Electrophoresis**, [S.L.], v. 15, n. 1, p. 529-539, jan. 1994. Wiley. http://dx.doi.org/10.1002/elps.1150150171.

BJELLQVIST, Bengt; HUGHES, Graham J.; PASQUALI, Christian; PAQUET, Nicole; RAVIER, Florence; SANCHEZ, Jean-Charles; FRUTIGER, Séverine; HOCHSTRASSER, Denis. The focusing positions of polypeptides in immobilized pH gradients can be predicted from their amino acid sequences. **Electrophoresis**, [S.L.], v. 14, n. 1, p. 1023-1031, jan. 1993. Wiley. http://dx.doi.org/10.1002/elps.11501401163.

BOLTON, Melvin D.. Primary Metabolism and Plant Defense—Fuel for the Fire. **Molecular Plant-Microbe Interactions®**, [S.L.], v. 22, n. 5, p. 487-497, maio 2009. Scientific Societies. http://dx.doi.org/10.1094/mpmi-22-5-0487.

CAMARÇO, Rosa Felicia E. Araújo; NASCIMENTO, Aline K. Queiroz do; ANDRADE, Eduardo C. de; LIMA, José Albersio A.. Biological, serological and molecular comparison between isolates of Cowpea severe mosaic virus. **Tropical Plant Pathology**, [S.L.], v. 34, n. 4, p. 239-244, ago. 2009. FapUNIFESP (SciELO). http://dx.doi.org/10.1590/s1982-56762009000400006.

CARVALHO, Márcia; CASTRO, Isaura; MOUTINHO-PEREIRA, José; CORREIA, Carlos; EGEA-CORTINES, Marcos; MATOS, Manuela; ROSA, Eduardo; CARNIDE, Valdemar; LINO-NETO, Teresa. Evaluating stress responses in cowpea under drought stress. **Journal Of Plant Physiology**, [S.L.], v. 241, p. 153001, out. 2019. Elsevier BV. http://dx.doi.org/10.1016/j.jplph.2019.153001.

COSTA, Alex; DRAGO, Ilaria; BEHERA, Smrutisanjita; ZOTTINI, Michela; PIZZO, Paola; SCHROEDER, Julian I.; POZZAN, Tullio; LOSCHIAVO, Fiorella. H2O2 in plant peroxisomes: an in vivo analysis uncovers a ca2+-dependent scavenging system. **The Plant Journal**, [S.L.], v. 62, n. 5, p. 760-772, 2 mar. 2010. Wiley. http://dx.doi.org/10.1111/j.1365-313x.2010.04190.x.

CUI, Li-Li; LU, Yu-Sheng; LI, Yong; YANG, Chengwei; PENG, Xin-Xiang. Overexpression of Glycolate Oxidase Confers Improved Photosynthesis under High Light and High Temperature in Rice. **Frontiers In Plant Science**, [S.L.], v. 7, p. 1-12, 4 ago. 2016. Frontiers Media SA. http://dx.doi.org/10.3389/fpls.2016.01165.

DANGL, Jeffery L.; HORVATH, Diana M.; STASKAWICZ, Brian J.. Pivoting the Plant Immune System from Dissection to Deployment. **Science**, [S.L.], v. 341, n. 6147, p. 746-

751, 16 ago. 2013. American Association for the Advancement of Science (AAAS). http://dx.doi.org/10.1126/science.1236011.

DAUDI, A.; O'BRIEN, J. Detection of Hydrogen Peroxide by DAB Staining in Arabidopsis Leaves. **BIO-PROTOCOL**, v. 2, n. 18, 2012.

DURAIPANDIAN, M.; POORANI, K.e.; ABIRAMI, H.; ANUSHA, M.B.. Vigna unguiculata (L.) Walp:: a strategic crop for nutritional security, well being and environmental protection. In: JIMENEZ-LOPE, Jose C. *et al*. **Legumes Research**: volume 2. 2. ed. [N.S]: Intechopen, 2022. Cap. 2, p. 372. Disponível em: https://www.intechopen.com/books/12236. Acesso em: 27 mar. 2026.

ENGQVIST, Martin K.M.; SCHMITZ, Jessica; GERTZMANN, Anke; FLORIAN, Alexandra; JASPERT, Nils; ARIF, Muhammad; BALAZADEH, Salma; MUELLER-ROEBER, Bernd; FERNIE, Alisdair R.; MAURINO, Veronica G.. GLYCOLATE OXIDASE3, a Glycolate Oxidase Homolog of Yeast l-Lactate Cytochrome c Oxidoreductase, Supports l-Lactate Oxidation in Roots of Arabidopsis. **Plant Physiology**, [S.L.], v. 169, n. 2, p. 1042-1061, 5 ago. 2015. Oxford University Press (OUP). http://dx.doi.org/10.1104/pp.15.01003.

FOYER, Christine H.; BLOOM, Arnold J.; QUEVAL, Guillaume; NOCTOR, Graham. Photorespiratory Metabolism: genes, mutants, energetics, and redox signaling. **Annual Review Of Plant Biology**, [S.L.], v. 60, n. 1, p. 455-484, 1 jun. 2009. Annual Reviews. http://dx.doi.org/10.1146/annurev.arplant.043008.091948.

FUCHS, Marc; HILY, Jean-Michel; PETRZIK, Karel; SANFAÇON, Hélène; THOMPSON, Jeremy R.; VLUGT, René van Der; WETZEL, Thierry. ICTV Virus Taxonomy Profile: secoviridae 2022. **Journal Of General Virology**, [S.L.], v. 103, n. 12, p. 1-2, 20 dez. 2022. Microbiology Society. http://dx.doi.org/10.1099/jgv.0.001807.

FUJIMOTO, Susan Y.; OHTA, Masaru; USUI, Akemi; SHINSHI, Hideaki; OHME-TAKAGI, Masaru. Arabidopsis Ethylene-Responsive Element Binding Factors Act as Transcriptional Activators or Repressors of GCC Box–Mediated Gene Expression. **The Plant Cell**, [S.L.], v. 12, n. 3, p. 393-404, mar. 2000. Oxford University Press (OUP). http://dx.doi.org/10.1105/tpc.12.3.393.

GASTEIGER, Elisabeth; HOOGLAND, Christine; GATTIKER, Alexandre; DUVAUD, S'Everine; WILKINS, Marc R.; APPEL, Ron D.; BAIROCH, Amos. Protein

Identification and Analysis Tools on the ExPASy Server. **The Proteomics Protocols Handbook**, [S.L.], p. 571-607, 2005. Humana Press. http://dx.doi.org/10.1385/1-59259-890-0:571.

GECHEV, Tsanko S.; VAN BREUSEGEM, Frank; STONE, Julie M.; DENEV, Iliya; LALOI, Christophe. Reactive oxygen species as signals that modulate plant stress responses and programmed cell death. **Bioessays**, [S.L.], v. 28, n. 11, p. 1091-1101, 2006. Wiley. http://dx.doi.org/10.1002/bies.20493.

GOMES, Ana M.F.; RODRIGUES, Ana P.; ANTÓNIO, Carla; RODRIGUES, Ana M.; LEITÃO, António E.; BATISTA-SANTOS, Paula; NHANTUMBO, Nascimento; MASSINGA, Rafael; RIBEIRO-BARROS, Ana I.; RAMALHO, José C.. Drought response of cowpea (Vigna unguiculata (L.) Walp.) landraces at leaf physiological and metabolite profile levels. **Environmental And Experimental Botany**, [S.L.], v. 175, p. 104060, jul. 2020. Elsevier BV. http://dx.doi.org/10.1016/j.envexpbot.2020.104060.

GOODSTEIN, David M.; SHU, Shengqiang; HOWSON, Russell; NEUPANE, Rochak; HAYES, Richard D.; FAZO, Joni; MITROS, Therese; DIRKS, William; HELLSTEN, Uffe; PUTNAM, Nicholas. Phytozome: a comparative platform for green plant genomics. **Nucleic Acids Research**, [S.L.], v. 40, n. 1, p. 1178-1186, 22 nov. 2011. Oxford University Press (OUP). http://dx.doi.org/10.1093/nar/gkr944.

HALL, N.P.; REGGIANI, R.; LEA, P.J.. Molecular weights of glycollate oxidase from C3 and C4 plants determined during early stages of purification. **Phytochemistry**, [S.L.], v. 24, n. 8, p. 1645-1648, jan. 1985. Elsevier BV. http://dx.doi.org/10.1016/s0031-9422(00)82527-3.

JAYAWARDHANE, Jayamini; GOYALI, Juran C.; ZAFARI, Somaieh; IGAMBERDIEV, Abir U.. The Response of Cowpea (Vigna unguiculata) Plants to Three Abiotic Stresses Applied with Increasing Intensity: hypoxia, salinity, and water deficit. **Metabolites**, [S.L.], v. 12, n. 1, p. 38, 4 jan. 2022. MDPI AG. http://dx.doi.org/10.3390/metabo12010038.

JONES, Jonathan D. G.; DANGL, Jeffery L.. The plant immune system. **Nature**, [S.L.], v. 444, n. 7117, p. 323-329, nov. 2006. Springer Science and Business Media LLC. http://dx.doi.org/10.1038/nature05286.

JONES, Jonathan D.G.; STASKAWICZ, Brian J.; DANGL, Jeffery L.. The plant immune system: from discovery to deployment. **Cell**, [S.L.], v. 187, n. 9, p. 2095-2116, abr. 2024. Elsevier BV. http://dx.doi.org/10.1016/j.cell.2024.03.045.

KANG, Lihua; TENG, Yangyang; CEN, Qiwen; FANG, Yunxia; TIAN, Quanxiang; ZHANG, Xiaoqin; WANG, Hua; ZHANG, Xian; XUE, Dawei. Genome-Wide Identification of R2R3-MYB Transcription Factor and Expression Analysis under Abiotic Stress in Rice. **Plants**, [S.L.], v. 11, n. 15, p. 1928, 25 jul. 2022. MDPI AG. http://dx.doi.org/10.3390/plants11151928.

KANGASJARVI, S.; NEUKERMANS, J.; LI, S.; ARO, E.-M.; NOCTOR, G.. Photosynthesis, photorespiration, and light signalling in defence responses. **Journal Of Experimental Botany**, [S.L.], v. 63, n. 4, p. 1619-1636, 25 jan. 2012. Oxford University Press (OUP). http://dx.doi.org/10.1093/jxb/err402.

KATAGIRI, Fumiaki; TSUDA, Kenichi. Understanding the Plant Immune System. **Molecular Plant-Microbe Interactions®**, [S.L.], v. 23, n. 12, p. 1531-1536, dez. 2010. Scientific Societies. http://dx.doi.org/10.1094/mpmi-04-10-0099.

KAUR, Amritpreet; PATI, Pratap Kumar; PATI, Aparna Maitra; NAGPAL, Avinash Kaur. In-silico analysis of cis-acting regulatory elements of pathogenesis-related proteins of Arabidopsis thaliana and Oryza sativa. **Plos One**, [S.L.], v. 12, n. 9, p. e0184523, 14 set. 2017. Public Library of Science (PLoS). http://dx.doi.org/10.1371/journal.pone.0184523.

KERN, Ramona; BAUWE, Hermann; HAGEMANN, Martin. Evolution of enzymes involved in the photorespiratory 2-phosphoglycolate cycle from cyanobacteria via algae toward plants. **Photosynthesis Research**, [S.L.], v. 109, n. 1-3, p. 103-114, 11 jan. 2011. Springer Science and Business Media LLC. http://dx.doi.org/10.1007/s11120-010-9615-z.

KITAJIMA, Elliot W.. An annotated list of plant viruses and viroids described in Brazil (1926-2018). **Biota Neotropica**, [S.L.], v. 20, n. 2, p. e20190932, 2020. FapUNIFESP (SciELO). http://dx.doi.org/10.1590/1676-0611-bn-2019-0932.

KUMAR, Sudhir; STECHER, Glen; LI, Michael; KNYAZ, Christina; TAMURA, Koichiro. MEGA X: molecular evolutionary genetics analysis across computing

platforms. **Molecular Biology And Evolution**, [S.L.], v. 35, n. 6, p. 1547-1549, 2 maio 2018. Oxford University Press (OUP). http://dx.doi.org/10.1093/molbev/msy096.

LAEMMLI, U. K.. Cleavage of Structural Proteins during the Assembly of the Head of Bacteriophage T4. **Nature**, [S.L.], v. 227, n. 5259, p. 680-685, ago. 1970. Springer Science and Business Media LLC. http://dx.doi.org/10.1038/227680a0.

LAZAR, Ana; COLL, Anna; DOBNIK, David; BAEBLER, Špela; BEDINA-ZAVEC, Apolonija; ŝEL, Jana; GRUDEN, Kristina. Involvement of Potato (Solanum tuberosum L.) MKK6 in Response to Potato virus Y. **Plos One**, [S.L.], v. 9, n. 8, p. e104553, 11 ago. 2014. Public Library of Science (PLoS). http://dx.doi.org/10.1371/journal.pone.0104553.

LI, Ruixiang; ZHU, Fanding; DUAN, Dong. Function analysis and stress-mediated cis-element identification in the promoter region of VqMYB15. **Plant Signaling & Behavior**, [S.L.], v. 15, n. 7, p. 1773664, 30 maio 2020. Informa UK Limited. http://dx.doi.org/10.1080/15592324.2020.1773664.

LI, Xiangyang; CHEN, Linru; ZENG, Xiaoyue; WU, Kaixin; HUANG, Jiayu; LIAO, Mengmeng; XI, Yue; ZHU, Guohui; ZENG, Xiuying; HOU, Xuewen. Wounding induces a peroxisomal H2O2 decrease via glycolate oxidase-catalase switch dependent on glutamate receptor-like channel-supported Ca2+ signaling in plants. **The Plant Journal**, [S.L.], v. 116, n. 5, p. 1325-1341, 19 ago. 2023. Wiley. http://dx.doi.org/10.1111/tpj.16427.

LI, Xiangyang; LIAO, Mengmeng; HUANG, Jiayu; CHEN, Linru; HUANG, Haiyin; WU, Kaixin; PAN, Qing; ZHANG, Zhisheng; PENG, Xinxiang. Dynamic and fluctuating generation of hydrogen peroxide via photorespiratory metabolic channeling in plants. **The Plant Journal**, [S.L.], v. 112, n. 6, p. 1429-1446, 30 nov. 2022. Wiley. http://dx.doi.org/10.1111/tpj.16022.

LI, Xiangyang; LIAO, Mengmeng; HUANG, Jiayu; XU, Zheng; LIN, Zhanqiao; YE, Nenghui; ZHANG, Zhisheng; PENG, Xinxiang. Glycolate oxidase-dependent H2O2 production regulates IAA biosynthesis in rice. **Bmc Plant Biology**, [S.L.], v. 21, n. 1, p. 326, 6 jul. 2021. Springer Science and Business Media LLC. http://dx.doi.org/10.1186/s12870-021-03112-4.

LIMA, José Albersio Araujo; NASCIMENTO, Aline Kelly Queiroz do; SILVA, Ana Kelly Firmino da; ARAGÃO, Maria do Livramento. Biological stability of a strain of

Cowpea severe mosaic virus over 20 years. **Revista Ciência Agronômica**, [S.L.], v. 43, n. 1, p. 105-111, mar. 2012. FapUNIFESP (SciELO). http://dx.doi.org/10.1590/s1806-66902012000100013.

LIMA-MELO, Yugo; ALENCAR, Vicente T. C. B.; LOBO, Ana K. M.; SOUSA, Rachel H. V.; TIKKANEN, Mikko; ARO, Eva-Mari; SILVEIRA, Joaquim A. G.; GOLLAN, Peter J.. Photoinhibition of Photosystem I Provides Oxidative Protection During Imbalanced Photosynthetic Electron Transport in Arabidopsis thaliana. **Frontiers In Plant Science**, [S.L.], v. 10, p. 916, 12 jul. 2019. Frontiers Media SA. http://dx.doi.org/10.3389/fpls.2019.00916.

LIU, Yujie; WU, Wei; CHEN, Zhongzhou. Structures of glycolate oxidase from Nicotiana benthamiana reveal a conserved pH sensor affecting the binding of FMN. **Biochemical And Biophysical Research Communications**, [S.L.], v. 503, n. 4, p. 3050-3056, set. 2018. Elsevier BV. http://dx.doi.org/10.1016/j.bbrc.2018.08.092.

MANDADI, Kranthi K.; SCHOLTHOF, Karen-Beth G.. Plant Immune Responses Against Viruses: how does a virus cause disease?. **The Plant Cell**, [S.L.], v. 25, n. 5, p. 1489-1505, maio 2013. Oxford University Press (OUP). http://dx.doi.org/10.1105/tpc.113.111658.

MARTINS, L. M. V.; XAVIER, G. R.; RANGEL, F. W.; RIBEIRO, J. R. A.; NEVES, M. C. P.; MORGADO, L. B.; RUMJANEK, N. G.. Contribution of biological nitrogen fixation to cowpea: a strategy for improving grain yield in the semi-arid region of brazil. **Biology And Fertility Of Soils**, [S.L.], v. 38, n. 6, p. 333-339, 1 out. 2003. Springer Science and Business Media LLC. http://dx.doi.org/10.1007/s00374-003-0668-4.

MITTLER, Ron; VANDERAUWERA, Sandy; SUZUKI, Nobuhiro; MILLER, Gad; TOGNETTI, Vanesa B.; VANDEPOELE, Klaas; GOLLERY, Marty; SHULAEV, Vladimir; VAN BREUSEGEM, Frank. ROS signaling: the new wave?. **Trends In Plant Science**, [S.L.], v. 16, n. 6, p. 300-309, jun. 2011. Elsevier BV. http://dx.doi.org/10.1016/j.tplants.2011.03.007.

MIZOI, Junya; OHORI, Teppei; MORIWAKI, Takashi; KIDOKORO, Satoshi; TODAKA, Daisuke; MARUYAMA, Kyonoshin; KUSAKABE, Kazuya; OSAKABE, Yuriko; SHINOZAKI, Kazuo; YAMAGUCHI-SHINOZAKI, Kazuko. GmDREB2A;2, a

Canonical DEHYDRATION-RESPONSIVE ELEMENT-BINDING PROTEIN2-Type Transcription Factor in Soybean, Is Posttranslationally Regulated and Mediates Dehydration-Responsive Element-Dependent Gene Expression . **Plant Physiology**, [S.L.], v. 161, n. 1, p. 346-361, 14 nov. 2012. Oxford University Press (OUP). http://dx.doi.org/10.1104/pp.112.204875.

NEILL, S. Hydrogen peroxide signalling. **Current Opinion In Plant Biology**, [S.L.], v. 5, n. 5, p. 388-395, 1 out. 2002. Elsevier BV. http://dx.doi.org/10.1016/s1369-5266(02)00282-0.

NICHOLLS, Peter; FITA, Ignacio; LOEWEN, Peter C.. Enzymology and structure of catalases. **Advances In Inorganic Chemistry**, [S.L.], p. 51-106, 2000. Elsevier. http://dx.doi.org/10.1016/s0898-8838(00)51001-0.

NIU, Liangjie; ZHANG, Hang; WU, Zhaokun; WANG, Yibo; LIU, Hui; WU, Xiaolin; WANG, Wei. Modified TCA/acetone precipitation of plant proteins for proteomic analysis. **Plos One**, [S.L.], v. 13, n. 12, p. e0202238, 17 dez. 2018. Public Library of Science (PLoS). http://dx.doi.org/10.1371/journal.pone.0202238.

PANDEY, Prachi; RAMEGOWDA, Venkategowda; SENTHIL-KUMAR, Muthappa. Shared and unique responses of plants to multiple individual stresses and stress combinations: physiological and molecular mechanisms. **Frontiers In Plant Science**, [S.L.], v. 6, p. 723, 16 set. 2015. Frontiers Media SA. http://dx.doi.org/10.3389/fpls.2015.00723.

PEREIRA, Elenilda J.; CARVALHO, Lucia M. J.; DELLAMORA-ORTIZ, Gisela M.; CARDOSO, Flávio S. N.; CARVALHO, José L. V.; VIANA, Daniela S.; FREITAS, Sidinea C.; ROCHA, Maurisrael M.. Effects of cooking methods on the iron and zinc contents in cowpea (Vigna unguiculata) to combat nutritional deficiencies in Brazil. **Food & Nutrition Research**, [S.L.], v. 58, n. 1, p. 20694, jan. 2014. SNF Swedish Nutrition Foundation. http://dx.doi.org/10.3402/fnr.v58.20694.

PFAFFL, M. W.. A new mathematical model for relative quantification in real-time RT-PCR. **Nucleic Acids Research**, [S.L.], v. 29, n. 9, p. 45-45, 1 maio 2001. Oxford University Press (OUP). http://dx.doi.org/10.1093/nar/29.9.e45.

POUWELS, Jeroen; CARETTE, Jan E.; VAN LENT, Jan; WELLINK, Joan. Cowpea mosaic virus: effects on host cell processes. **Molecular Plant Pathology**, [S.L.], v. 3, n. 6, p. 411-418, 31 out. 2002. Wiley. http://dx.doi.org/10.1046/j.1364-3703.2002.00135.x.

QUEIROZ, Cinthia Silva de; PEREIRA, Isabelle Mary Costa; LIMA, Karollyny Roger Pereira; BRET, Raissa Souza Caminha; ALVES, Murilo Siqueira; GOMES-FILHO, Enéas; CARVALHO, Humberto Henrique de. Combined NaCl and DTT diminish harmful ER-stress effects in the sorghum seedlings CSF 20 variety. **Plant Physiology And Biochemistry**, [S.L.], v. 147, p. 223-234, fev. 2020. Elsevier BV. http://dx.doi.org/10.1016/j.plaphy.2019.12.013.

RASKIN, Ilya. Role of Salicylic acid in plants. **Annual Review of Plant Biology**, v. 43, p. 439–463, 1992.

RISEH, Roohallah Saberi; FATHI, Fariba; VATANKHAH, Masoumeh; KENNEDY, John F.. Catalase-associated immune responses in plant-microbe interactions: a review. **International Journal Of Biological Macromolecules**, [S.L.], v. 280, p. 135859, nov. 2024. Elsevier BV. http://dx.doi.org/10.1016/j.ijbiomac.2024.135859.

ROJAS, Clemencia M.; SENTHIL-KUMAR, Muthappa; TZIN, Vered; MYSORE, Kirankumar S.. Regulation of primary plant metabolism during plant-pathogen interactions and its contribution to plant defense. **Frontiers In Plant Science**, [S.L.], v. 5, p. 17, 2014. Frontiers Media SA. http://dx.doi.org/10.3389/fpls.2014.00017.

ROJAS, Clemencia M.; SENTHIL-KUMAR, Muthappa; WANG, Keri; RYU, Choong-Min; KAUNDAL, Amita; MYSORE, Kirankumar S.. Glycolate Oxidase Modulates Reactive Oxygen Species–Mediated Signal Transduction during Nonhost Resistance in Nicotiana benthamiana and Arabidopsis . **The Plant Cell**, [S.L.], v. 24, n. 1, p. 336-352, 1 jan. 2012. Oxford University Press (OUP). http://dx.doi.org/10.1105/tpc.111.093245.

ROQUE, Érica Monik Silva; TEIXEIRA, Felipe de Castro; AGUIAR, Alex Martins de; BEZERRA, Victor Breno Faustino; COSTA, Ana Carolina Moreira da; SILVA, Sâmia Alves; PAIVA, Ana Luiza Sobral; CARVALHO, Humberto Henrique de; ALVES, Murilo Siqueira. Genome-wide comparative analysis of Glycolate oxidase (GOX) gene family in plants. **Plant Gene**, [S.L.], v. 34, p. 100407, jun. 2023. Elsevier BV. http://dx.doi.org/10.1016/j.plgene.2023.100407.

SHARMA, Pallavi; JHA, Ambuj Bhushan; DUBEY, Rama Shanker; PESSARAKLI, Mohammad. Reactive Oxygen Species, Oxidative Damage, and Antioxidative Defense Mechanism in Plants under Stressful Conditions. **Journal Of Botany**, [S.L.], v. 2012, p. 1-26, 24 abr. 2012. Wiley. http://dx.doi.org/10.1155/2012/217037.

SOUZA, Pedro F. N.; SILVA, Fredy D. A.; CARVALHO, Fabricio E. L.; SILVEIRA, Joaquim A. G.; VASCONCELOS, Ilka M.; OLIVEIRA, Jose T. A.. Photosynthetic and biochemical mechanisms of an EMS-mutagenized cowpea associated with its resistance to cowpea severe mosaic virus. **Plant Cell Reports**, [S.L.], v. 36, n. 1, p. 219-234, 12 nov. 2016. Springer Science and Business Media LLC. http://dx.doi.org/10.1007/s00299-016-2074-z.

SOUZA, Pedro Filho Noronha; OLIVEIRA, Jose Tadeu Abreu; VASCONCELOS, Ilka Maria; MAGALHÃES, Vladimir Gonçalves; SILVA, Fredy Davi Albuquerque; SILVA, Rodolpho Glauber Guedes; OLIVEIRA, Kleber Sousa; FRANCO, Octavio Luis; SILVEIRA, Joaquim Albenisio Gomes; CARVALHO, Fabricio Eulalio Leite. H2O2Accumulation, Host Cell Death and Differential Levels of Proteins Related to Photosynthesis, Redox Homeostasis, and Required for Viral Replication Explain the Resistance of EMS-mutagenized Cowpea to Cowpea Severe Mosaic Virus. **Journal Of Plant Physiology**, [S.L.], v. 245, p. 153110, fev. 2020. Elsevier BV. http://dx.doi.org/10.1016/j.jplph.2019.153110.

SOUZA, Pedro Filho Noronha; OLIVEIRA, Jose Tadeu Abreu; VASCONCELOS, Ilka Maria; MAGALHÃES, Vladimir Gonçalves; SILVA, Fredy Davi Albuquerque; SILVA, Rodolpho Glauber Guedes; OLIVEIRA, Kleber Sousa; FRANCO, Octavio Luis; SILVEIRA, Joaquim Albenisio Gomes; CARVALHO, Fabricio Eulalio Leite. H2O2Accumulation, Host Cell Death and Differential Levels of Proteins Related to Photosynthesis, Redox Homeostasis, and Required for Viral Replication Explain the Resistance of EMS-mutagenized Cowpea to Cowpea Severe Mosaic Virus. **Journal Of Plant Physiology**, [S.L.], v. 245, p. 153110, fev. 2020. Elsevier BV. http://dx.doi.org/10.1016/j.jplph.2019.153110.

TEIXEIRA, Kelvin Josemar M. L.; CASCARDO, Renan de Souza; LEAL, Lorhan L.; ZERBINI, F. Murilo; BESERRA, José Evando A.. First complete genome sequence of an isolate of cowpea severe mosaic virus from South America. **Virus Genes**, [S.L.], v.

57, n. 2, p. 238-241, 8 fev. 2021. Springer Science and Business Media LLC. http://dx.doi.org/10.1007/s11262-021-01831-2.

THOMPSON, Jeremy R; DASGUPTA, Indranil; FUCHS, Marc; IWANAMI, Toru; KARASEV, Alexander V; PETRZIK, Karel; SANFAÇON, Hélène; TZANETAKIS, Ioannis; VLUGT, René van Der; WETZEL, Thierry. ICTV Virus Taxonomy Profile: secoviridae. **Journal Of General Virology**, [S.L.], v. 98, n. 4, p. 529-531, 1 abr. 2017. Microbiology Society. http://dx.doi.org/10.1099/jgv.0.000779.

VARELA, Anna Lídia Nunes; OLIVEIRA, Jose Tadeu Abreu; KOMATSU, Setsuko; SILVA, Rodolpho Glauber Guedes; MARTINS, Thiago Fernandes; SOUZA, Pedro Filho Noronha; LOBO, Ana Karla Moreira; VASCONCELOS, Ilka Maria; CARVALHO, Fabricio Eulálio Leite; SILVEIRA, Joaquim Albenisio Gomes. A resistant cowpea (Vigna unguiculata [L.] Walp.) genotype became susceptible to cowpea severe mosaic virus (CPSMV) after exposure to salt stress. **Journal Of Proteomics**, [S.L.], v. 194, p. 200-217, mar. 2019. Elsevier BV. http://dx.doi.org/10.1016/j.jprot.2018.11.015.

VELIKOVA, V; YORDANOV, I; A EDREVA,. Oxidative stress and some antioxidant systems in acid rain-treated bean plants. **Plant Science**, [S.L.], v. 151, n. 1, p. 59-66, fev. 2000. Elsevier BV. http://dx.doi.org/10.1016/s0168-9452(99)00197-1.

WALKER, Peter J.; SIDDELL, Stuart G.; LEFKOWITZ, Elliot J.; MUSHEGIAN, Arcady R.; ADRIAENSSENS, Evelien M.; DEMPSEY, Donald M.; DUTILH, Bas E.; HARRACH, Balázs; HARRISON, Robert L.; HENDRICKSON, R. Curtis. Changes to virus taxonomy and the Statutes ratified by the International Committee on Taxonomy of Viruses (2020). **Archives Of Virology**, [S.L.], v. 165, n. 11, p. 2737-2748, 20 ago. 2020. Springer Science and Business Media LLC. http://dx.doi.org/10.1007/s00705-020-04752-x.

WINGLER, Astrid; LEA, Peter J.; QUICK, W. Paul; LEEGOOD, Richard C.. Photorespiration: metabolic pathways and their role in stress protection. **Philosophical Transactions Of The Royal Society Of London. Series B**: Biological Sciences, [S.L.], v. 355, n. 1402, p. 1517-1529, 29 out. 2000. The Royal Society. http://dx.doi.org/10.1098/rstb.2000.0712.

WU, Qiang Sheng; ZOU, Ying Ning; XIA, Ren Xue. Effects of water stress and arbuscular mycorrhizal fungi on reactive oxygen metabolism and antioxidant

production by citrus (Citrus tangerine) roots. **European Journal Of Soil Biology**, [S.L.], v. 42, n. 3, p. 166-172, jul. 2006. Elsevier BV. http://dx.doi.org/10.1016/j.ejsobi.2005.12.006.

YANG, Meng; LI, Zhenggang; ZHANG, Kun; ZHANG, Xuan; ZHANG, Yongliang; WANG, Xianbing; HAN, Chenggui; YU, Jialin; XU, Kai; LI, Dawei. Barley Stripe Mosaic Virus γb Interacts with Glycolate Oxidase and Inhibits Peroxisomal ROS Production to Facilitate Virus Infection. **Molecular Plant**, [S.L.], v. 11, n. 2, p. 338-341, fev. 2018. Elsevier BV. http://dx.doi.org/10.1016/j.molp.2017.10.007.

ZHANG, Zhisheng; LU, Yusheng; ZHAI, Liguang; DENG, Rongshu; JIANG, Jun; LI, Yong; HE, Zhenghui; PENG, Xinxiang. Glycolate Oxidase Isozymes Are Coordinately Controlled by GLO1 and GLO4 in Rice. **Plos One**, [S.L.], v. 7, n. 6, p. e39658, 26 jun. 2012. Public Library of Science (PLoS). http://dx.doi.org/10.1371/journal.pone.0039658.

.

Supplementary Tables:

Supplementary Table 1. List of genes used for quantification of gene expression by qPCR and the reference genes. Primer sequences of *V. unguiculata* reference and target genes, gene product description, amplicon size, accession number at Phytozome database, and optimal melting temperature (Tm) of each oligonucleotide.

Gene	ID	Gene Product	Primer Sequence	Amplicon (bp)	Fw/Rv Tm (°C)
GOX1	*Vigun01g052400*		**Fw**: TACCCCAAGACTAGGACGCA	**112**	**60/60**
			Rv: CGCTCAATGCCATGGTTAGC		
GOX2	*Vigun03g162000*		**Fw:** GCCCTTACTGTGGACACTCC	**513**	**60/61**
			Rv: CACACCAGCCTCTCCATCAG		
GOX3	*VigunL052501*		**Fw:** AAGCACGATGAACGCGAATG	**685**	**59.9/59.9**
			Rv: GGGCCAGAAACCCCGTATAG		
CATa	*Vigun09g260100*		**Fw:** CCGGAGAGCCTTCACATGTT	**530**	**60/60**
			Rv: AGCCTGTGCCTCTGTGAATC		

CA Tb	*Vigun08g00 1400*	**Fw:** ACCTGTGCTGACTTCCTTCG	**518**	**60/60**
		Rv: TCGTAAAGGTCTTGGGTGGC		
CA Tc	*Vigun05g26 4800*	**Fw:** CTTGTGTGTGGACTTGCTGC	**574**	**60/60**
		Rv: AGGCACTTTGGGTGTTGGAA		
MP	*MW392574*	**Fw:** GGGGGGATCCATGTCAACATT TCGTTACAGG	**599**	**60/60. 1**
		Rv: GGGGGAATTCTCAATACTGAA TGTATCCTGT		
UB Q3	*Vigun03g10 5700.2*	**Fw:** TCTTGTCTTGCGACTCCGTG	**90**	**60/60**
		Rv: TCGTGTCTGAACTCTCGACC		

Supplementary Table 2. List of all cis-elements found in the promoter region of Glycolate Oxidase (GOX) and Catalase (CAT) from *V. unguiculata*, showing cis-element identification, class, and description

Gene ID	***Cis-element* Class**	***Cis-element* description**
CATa	CAAT-box	common cis-acting element in promoter and enhancer regions
CATa	CAAT-box	
CATa	WUN-motif	part of a conserved DNA module involved in light responsiveness
CATa	Box 4	
CATa	ERE	

CATa	GARE-motif	gibberellin-responsive element
CATa	TCA	
CATa		Myb-binding site
CATa		AAGAA-motif
CATa	TATC-box	cis-acting element involved in gibberellin-responsiveness
CATa	GA-motif	part of a light responsive element
CATa	TATA	
CATa		AT~TATA-box
CATa	Myc	
CATa	TATA-box	core promoter element around -30 of transcription start
CATa	circadian	cis-acting regulatory element involved in circadian control
CATa		short_function
CATa	AP-1	
CATa	MYB	
CATa		MYB-like sequence
CATa	ATCT-motif	part of a conserved DNA module involved in light responsiveness
CATa	ARE	cis-acting regulatory element essential for the anaerobic induction
CATb	Myb	
CATb	Box 4	part of a conserved DNA module involved in light responsiveness
CATb	CAAT-box	
CATb	CAAT-box	common cis-acting element in promoter and enhancer regions
CATb		short_function
CATb	TCT-motif	part of a light responsive element
CATb	ERE	
CATb	F-box	
CATb	MYC	
CATb	Unnamed__1	60K protein binding site

		part of a conserved DNA module involved in light
CATb	ATCT-motif	responsiveness
CATb	TATA	
CATb	chs-CMA1a	part of a light responsive element
CATb	P-box	gibberellin-responsive element
CATb		AT~TATA-box
CATb	GATA-motif	part of a light responsive element
CATb	STRE	
CATb	GT1-motif	light responsive element
CATb	TATA-box	core promoter element around -30 of transcription start
		part of a conserved DNA module involved in light
CATc	Box 4	responsiveness
CATc	CAAT-box	
		common cis-acting element in promoter and enhancer
CATc	CAAT-box	regions
		cis-acting element involved in low-temperature
CATc	LTR	responsiveness
CATc	TCT-motif	part of a light responsive element
CATc	ERE	
CATc	ABRE4	
CATc		Myb-binding site
		cis-acting regulatory element involved in light
CATc	G-Box	responsiveness
CATc	MYC	
CATc	TGA-element	auxin-responsive element
CATc		AAGAA-motif
CATc		AT~TATA-box
CATc	GA-motif	part of a light responsive element
CATc	TATA-box	core promoter element around -30 of transcription start
		MYB binding site involved in flavonoid biosynthetic
CATc	MBSI	genes regulation
		cis-acting element involved in the abscisic acid
CATc	ABRE	responsiveness

CATc	ABRE3a	
CATc		short_function
CATc	TC-rich repeats	cis-acting element involved in defense and stress responsiveness
CATc	MYB	
CATc		MYB-like sequence
CATc	ARE	cis-acting regulatory element essential for the anaerobic induction
CATc	GATA-motif	part of a light responsive element
CATc	GT1-motif	light responsive element
GOX1		MYB-like sequence
GOX1		Unnamed__4
GOX1	as-1	
GOX1	GT1-motif	light responsive element
GOX1	P-box	gibberellin-responsive element
GOX1	G-box	cis-acting regulatory element involved in light responsiveness
GOX1	ARE	cis-acting regulatory element essential for the anaerobic induction
GOX1	MRE	MYB binding site involved in light responsiveness
GOX1	TGACG-motif	cis-acting regulatory element involved in the MeJA-responsiveness
GOX1	TC-rich repeats	cis-acting element involved in defense and stress responsiveness
GOX1	MYB	
GOX1		short_function
GOX1	WRE3	
GOX1	CAT-box	cis-acting regulatory element related to meristem expression
GOX1	DRE1	
GOX1		Unnamed__6
GOX1	TATA-box	core promoter element around -30 of transcription start

GOX1	MBSI	MYB binding site involved in flavonoid biosynthetic genes regulation
GOX1	Myc	
GOX1	ABRE	cis-acting element involved in the abscisic acid responsiveness
GOX1	STRE	
GOX1		AT~TATA-box
GOX1	TATA	
GOX1	GA-motif	part of a light responsive element
GOX1	CAAT-box	
GOX1	CAAT-box	common cis-acting element in promoter and enhancer regions
GOX1	Box 4	part of a conserved DNA module involved in light responsiveness
GOX1	TCA-element	cis-acting element involved in salicylic acid responsiveness
GOX1	CGTCA-motif	cis-acting regulatory element involved in the MeJA-responsiveness
GOX1	ERE	
GOX1	TCT-motif	part of a light responsive element
GOX2	AT1-motif	part of a light responsive module
GOX2	LAMP-element	part of a light responsive element
GOX2	as-1	
GOX2	CCAAT-box	MYBHv1 binding site
GOX2		Unnamed__4
GOX2	AT-rich element	binding site of AT-rich DNA binding protein (ATBP-1)
GOX2	MRE	MYB binding site involved in light responsiveness
GOX2	P-box	gibberellin-responsive element
GOX2	G-box	cis-acting regulatory element involved in light responsiveness
GOX2	TGACG-motif	cis-acting regulatory element involved in the MeJA-responsiveness
GOX2	MBS	MYB binding site involved in drought-inducibility

GOX2	MYB	
GOX2		short_function
GOX2	box S	
GOX2	ABRE3a	
GOX2		AAGAA-motif
GOX2	MYC	
GOX2		MYB recognition site
GOX2	ABRE	cis-acting element involved in the abscisic acid responsiveness
GOX2	TATA-box	core promoter element around -30 of transcription start
GOX2		ACTCATCCT sequence
GOX2		AT~TATA-box
GOX2	CAAT-box	common cis-acting element in promoter and enhancer regions
GOX2	CAAT-box	
GOX2	Box 4	part of a conserved DNA module involved in light responsiveness
GOX2	WUN-motif	
GOX2	AE-box	part of a module for light response
GOX2	ABRE4	
GOX2	3-AF3 binding site	part of a conserved DNA module array (CMA3)
GOX2	CGTCA-motif	cis-acting regulatory element involved in the MeJA-responsiveness
GOX2	TCT-motif	part of a light responsive element
GOX2	ERE	

Supplementary Table 3. List of all accession and parameters from sub-cellular prediction tools CELLO of Glycolate Oxidase (GOX) and Catalase (CAT) proteins from *V. unguiculata*, and identity with *Arabidospsis thaliana* catalase from the Phytozome v13 database BlastP tool.

Gene	Protein	Locus name	*A. thaliana* Protein	Identity (%)	CELLO		
						Localization	Reability
VuCATa	VuCATa.1	Vigun08g001400.1	AT1G20630.1	85	Amino Acid Comp.	Peroxisomal	0.660
					N-peptide Comp.	Peroxisomal	0.885
					Partitioned seq. Comp.	Peroxisomal	0.700
					Physico-chemical Comp.	Peroxisomal	0.845
					Neighboring seq. Comp.	Peroxisomal	0.679
					CELLO Prediction	Peroxisomal	3.769
						Cytoplasmic	0.370
						Mitochondrial	0.344
						Extracellular	0.113
						Chloroplast	0.109
						Nuclear	0.103
						ER	0.050
						PlasmaMembrane	0.041

						Lysosomal	0.034
						Cytoskeletal	0.027
						Vacuole	0.022
						Golgi	0.017
VuCATb	VuCATb.1	Vigun09g260100.1	AT4G35090.1	86	Amino Acid Comp.	Peroxisomal	0.798
					N-peptide Comp.	Peroxisomal	0.901
VuGOX1	VuGOX1.1 VuGOX1.2 VuGOX1.3	Vigun01g052400	-	-	Partitioned seq. Comp.	Peroxisomal	0.742
					Physico-chemical Comp.	Peroxisomal	0.909
					Neighboring seq. Comp.	Peroxisomal	0.821
					CELLO Prediction:	Peroxisomal	4.171
						Mitochondrial	0.242
						Cytoplasmic	0.225

						Chloroplast	0.076
						Extracellular	0.063
						Nuclear	0.063
						ER	0.048
						Vacuole	0.025
						PlasmaMembrane	0.023
						Golgi	0.022
						Lysosomal	0.022
						Cytoskeletal	0.020
VuGOX2	VuGOX2.1	Vigun03g162000	-	-	Amino Acid Comp.	Mitochondrial	0.277
	VuGOX2.2				N-peptide Comp.	Peroxisomal	0.591
	VuGOX2.3				Partitioned seq. Comp.	Peroxisomal	0.721
	VuGOX2.4				Physico-chemical Comp.	Peroxisomal	0.509
	VuGOX2.5						
	VuGOX2.6				Neighboring seq. Comp.	Peroxisomal	0.657

					CELLO Prediction:	Peroxisomal	4.171
						Mitochondrial	0.242
						Cytoplasmic	0.225
						Chloroplast	0.076
						Extracellular	0.063
						Nuclear	0.063
						ER	0.048
						Vacuole	0.025
						PlasmaMembrane	0.023
						Golgi	0.022
						Lysosomal	0.022
						Cytoskeletal	0.020
VuGOX3	VuGOX3.1	VigunL052501	-	-	Amino Acid Comp.	Mitochondrial	0.407
					N-peptide Comp.	Mitochondrial	0.576
					Partitioned seq. Comp.	PlasmaMembrane	0.416
					Physico-chemical Comp.	Cytoplasmic	0.501

Neighboring seq. Comp.	Chloroplast	0.393
CELLO Prediction:	Mitochondrial	1.573
	Cytoplasmatic	0.880
	Chloroplast	0.780
	PlasmaMembrane	0.695
	Peroxisomal	0.538
	Nuclear	0.217
	Extracellular	0.151
	Vacuole	0.062
	Lysosomal	0.031
	ER	0.029
	Cytoskeletal	0.025
	Golgi	0.018

Supplementary Figures:

Supplementary Figure 1. Mock and Infected with Cowpea Severe Mosaic Virus (CPSMV) *V. unguiculata* leaves after 14 days maintained at greenhouse condition, from both cultivars Mock Pitiúba (a), infected Pitiúba (b), Mock Macaibo (c), and infected Macaibo (d).

VuCATa. V.unguiculata v1.2|Vigun08g001400.1.p

id	site	distance	identity	comments
CAT1_GOSHI	pero	93.8833	88.6179%	[Uniprot] SWISS-PROT45:Peroxisomal.
CAT1_CUCPE	pero	96.1504	87.8049%	[Uniprot] SWISS-PROT45:Glyoxysomal.
CAT2_ARATH	pero	100.7	85.7724%	[Uniprot] SWISS-PROT45:Peroxisomal and glyoxysomal.
CATA_IPOBA	pero	117.829	79.065%	[Uniprot] SWISS-PROT45:Peroxisomal.
CAT1_MAIZE	pero	120.45	82.7236%	[Uniprot] SWISS-PROT45:Peroxisomal.
CATA_PEA	pero	142.276	86.8421%	[Uniprot] SWISS-PROT45:Peroxisomal.
At1g20620.1	pero	158.489	78.252%	[Arath]
At1g77760.1	cyto	176.939	13.0862%	[Arath]
G6PC_SOLTU	chlo	272.508	14.3847%	[Uniprot] SWISS-PROT45:Chloroplast.
AROK_LYCES	chlo	277.883	14.8374%	[Uniprot] SWISS-PROT45:Chloroplast.
SQD1_SPIOL	chlo	280.154	11.0442%	[Uniprot] SWISS-PROT45:Chloroplast stroma.
GPD2_ARATH	chlo	289.676	15.4362%	[Uniprot] SWISS-PROT45:Chloroplast.
GCST_FLATR	mito	293.076	12.6016%	[Uniprot] SWISS-PROT45:Mitochondrial.
At1g20630.1	pero	302.227	85.3659%	[Arath]

VuCATb. V.unguiculata v1.2|Vigun09g260100.1.p

id	site	distance	identity	comments
CATA_PEA	pero	45.1277	87.8543%	[Uniprot] SWISS-PROT45:Peroxisomal.
CAT1_CUCPE	pero	69.2564	87.8049%	[Uniprot] SWISS-PROT45:Glyoxysomal.
CAT1_GOSHI	pero	81.8812	90.6504%	[Uniprot] SWISS-PROT45:Peroxisomal.
CAT1_MAIZE	pero	105.412	81.9106%	[Uniprot] SWISS-PROT45:Peroxisomal.
CATA_IPOBA	pero	109.178	77.0325%	[Uniprot] SWISS-PROT45:Peroxisomal.
CAT2_ARATH	pero	115.753	86.1789%	[Uniprot] SWISS-PROT45:Peroxisomal and glyoxysomal.
At1g20620.1	pero	177.326	77.0325%	[Arath]
GCST_FLATR	mito	258.099	12.5761%	[Uniprot] SWISS-PROT45:Mitochondrial.
At1g77760.1	cyto	262.755	14.0676%	[Arath]
GPD2_ARATH	chlo	281.697	14.7651%	[Uniprot] SWISS-PROT45:Chloroplast.
GCST_SOLTU	mito	283.345	12.3732%	[Uniprot] SWISS-PROT45:Mitochondrial.
GCST_FLAAN	mito	284.315	12.9817%	[Uniprot] SWISS-PROT45:Mitochondrial.
DAP1_WHEAT	chlo	285.138	13.8211%	[Uniprot] SWISS-PROT45:Chloroplast.
SQD1_SPIOL	chlo	285.853	12.0724%	[Uniprot] SWISS-PROT45:Chloroplast stroma.

VuGOX1. V.unguiculata v1.2|Vigun01g052400.1.p

id	site	distance	identity	comments
GOX_SPIOL	pero	158.199	89.5161%	[Uniprot] SWISS-PROT45:Peroxisomal.
ALFD_PEA	chlo	166.146	10.9626%	[Uniprot] SWISS-PROT45:Chloroplast.
ENO_ALNGL	cyto	189.671	14.7392%	[Uniprot] SWISS-PROT45:Cytoplasmic.
KADC_MAIZE	chlo	194.341	12.9032%	[Uniprot] SWISS-PROT45:Chloroplast.
MDHG_ORYSA	pero	214.317	11.0215%	[Uniprot] SWISS-PROT45:Glyoxysomal.
ADT1_SOLTU	mito	221.04	13.1783%	[Uniprot] SWISS-PROT45:Integral membrane protein. Mitochondrial inner membrane.
ERFA_ARATH	cyto	222.618	15.1376%	[Uniprot] SWISS-PROT45:Cytoplasmic.
ALF1_PEA	cyto	224.352	13.9474%	[Uniprot] SWISS-PROT45:Cytoplasmic.
ERFC_ARATH	cyto	228.389	13.5632%	[Uniprot] SWISS-PROT45:Cytoplasmic.
ALF_ARATH	cyto	234.451	13.6729%	[Uniprot] SWISS-PROT45:Cytoplasmic.
MDHG_SOYBN	pero	236.474	14.7453%	[Uniprot] SWISS-PROT45:Glyoxysomal.
MDHH_BRANA	pero	245.806	12.3656%	[Uniprot] SWISS-PROT45:Glyoxysomal.
MDHG_BRANA	pero	247.64	12.3656%	[Uniprot] SWISS-PROT45:Glyoxysomal.
ENO1_MAIZE	cyto	247.792	15.4362%	[Uniprot] SWISS-PROT45:Cytoplasmic.

VuGOX2. V.unguiculata v1.2|Vigun03g162000.5.p

id	site	distance	identity	comments
At1g75950.1	cysk_nucl	192.83	11.413%	[Arath]
GOX_SPIOL	pero	199.33	86.2162%	[Uniprot] SWISS-PROT45:Peroxisomal.
At4g26220.1	cyto	200.518	16.0326%	[Arath]
ENO_ALNGL	cyto	200.561	12.0455%	[Uniprot] SWISS-PROT45:Cytoplasmic.
At1g67990.1	cyto	210.356	13.0435%	[Arath]
MDHG_ORYSA	pero	213.751	10.0543%	[Uniprot] SWISS-PROT45:Glyoxysomal.
CYSK_SPIOL	cyto	222.373	15.6757%	[Uniprot] SWISS-PROT45:Cytoplasmic.
ALF_ARATH	cyto	222.748	13.0081%	[Uniprot] SWISS-PROT45:Cytoplasmic.
At1g63140.1	cyto	223.551	16.0326%	[Arath]
CB2_PHYPA	chlo	238.542	14.9457%	[Uniprot] SWISS-PROT45:Chloroplast thylakoid membrane.
PGKY_TOBAC	cyto	239.111	13.9303%	[Uniprot] SWISS-PROT45:Cytoplasmic.
MDHG_SOYBN	pero	239.596	14.8649%	[Uniprot] SWISS-PROT45:Glyoxysomal.
At1g21100.1	cyto	240.852	16.4491%	[Arath]
ALF_MAIZE	cyto	242.367	11.2903%	[Uniprot] SWISS-PROT45:Cytoplasmic.

VuGOX3. V.unguiculata v1.2|VigunL052501.1.p

id	site	distance	identity	comments
RIP3_MAIZE	cyto	252.169	14.2857%	[Uniprot] SWISS-PROT45:Cytoplasmic.
At1g46768.1	nucl	259.995	11.1688%	[Arath]
ALFC_SPIOL	chlo	262.279	12.3116%	[Uniprot] SWISS-PROT45:Chloroplast.
CB2_PHYPA	chlo	265.902	15.0649%	[Uniprot] SWISS-PROT45:Chloroplast thylakoid membrane.
RIP9_MAIZE	cyto	270.656	14.8052%	[Uniprot] SWISS-PROT45:Cytoplasmic.
CB23_POLMU	chlo	271.045	14.8052%	[Uniprot] SWISS-PROT45:Chloroplast thylakoid membrane.
ALFD_PEA	chlo	271.245	14.8052%	[Uniprot] SWISS-PROT45:Chloroplast.
CB2A_SPIOL	chlo	281.102	15.5844%	[Uniprot] SWISS-PROT45:Chloroplast thylakoid membrane.
CAP3_SORBI	cyto	282.513	11.9792%	[Uniprot] SWISS-PROT45:Cytoplasmic.
ALF_ARATH	cyto	283.042	12.1762%	[Uniprot] SWISS-PROT45:Cytoplasmic.
ALB3_MAIZE	cyto	284.742	15.0649%	[Uniprot] SWISS-PROT45:Cytoplasmic.
PGKY_TOBAC	cyto	291.364	10.2244%	[Uniprot] SWISS-PROT45:Cytoplasmic.
At5g62190.1	nucl	292.349	13.7109%	[Arath]
At2g35630.1	cysk	295.875	6.62285%	[Arath]

Supplementary Figure 1. List of all accession and parameters from sub-cellular prediction tools WoLFPSORT of Glycolate Oxidase (GOX) and Catalase (CAT) proteins from *V. unguiculata*, and identity with *Arabidospsis thaliana* catalase from the Phytozome v13 database BlastP tool.

ANEXO DE PRODUTIVIDADE

Plant Gene 39 (2024) 100459

Contents lists available at ScienceDirect

Plant Gene

journal homepage: www.elsevier.com/locate/plantgene

Apoptotic chromatin condensation inducer in the nucleus: Genome-wide analysis in plants and expression profile during Cowpea Severe Mosaic Virus infection in *Vigna unguiculata* [L.] Walp

Felipe Castro Teixeira [a], Erica Monik Silva Roque [a], Alex Martins Aguiar [a], Sâmia Alves Silva [a], Victor Breno Faustino Bezerra [a], Otávio Hugo Aguiar Gomes [a], Luciano Gomes Fietto [b], Murilo Siqueira Alves [a,*]

[a] Departamento de Bioquímica e Biologia Molecular, Universidade Federal do Ceará, Avenida Humberto Monte S/N, Campus do Pici, Fortaleza, CE 60440-900, Brasil
[b] Departamento de Bioquímica e Biologia Molecular, Universidade Federal de Viçosa, Avenida PH Rolfs S/N, Campus Viçosa, Viçosa, MG 36570-900, Brasil

ARTICLE INFO

Editor Name: Dr. Bingye Xue

Keywords:
ACIN1
Programmed cell death
Chromatin modulation
Plant phylogenetics
Synteny analysis
Differential expression

ABSTRACT

Apoptotic Chromatin Condensation Inducer in the Nucleus (ACIN1) is a scaffold protein that was first described as a complex component responsible for triggering apoptosis in human cells. In plants, ACIN1 participates in silencing of *Flowering Locus C* (*FLC*), involved in vernalization in *Arabidopsis thaliana*. Contrary to what has been observed for humans, there are no reports on ACIN1 linked to programmed cell death (PCD) in plants. Actually, the function of ACIN1 in plants is still poorly understood. In the present study, a genome-wide analysis of the *ACIN1* gene family in plants identified 27 *ACIN1* orthologs from 19 species belonging to 12 plant families. The phylogenetic relationships, physicochemical properties, gene structure, conserved motifs, promoter *cis*-elements, chromosomal localization, syntenic regions, and protein network were investigated. Altogether, these analyzes revealed highly conserved domains in the structure of the ACIN1 proteins, as well as putative metacaspase cleavage sites, which suggest that they play a conserved function probably associated with the programmed cell death in plants. For instance, differential expression pattern and modulation of *ACIN1* were noticed after inoculation of cowpea with Cowpea severe mosaic virus (CPSMV). Therefore, this study was conducted to provide, for the first time, information on the evolutionary, structural, and functional characteristics of the *ACIN1* gene family as an initial effort towards understanding the role of these proteins in studied plant development and stress responses.

1. Introduction

Programmed cell death (PCD) is a fundamental process for homeostasis maintenance in most living beings. It involves a plethora of molecular factors for its occurrence and regulation (Green, 2019; Kerr et al., 1972), one of these components is the Apoptotic Chromatin Condensation Inducer in the Nucleus (ACIN1, or ACINUS). ACIN1 is a well-known protein in animals since its functional role in humans is well documented (Deka and Singh, 2019; Michelle et al., 2012; Sahara et al., 1999). ACIN1 was first described by Sahara and collaborators as one of the proteins responsible for triggering one of the most known apoptosis pathways in *HeLa* cells (Sahara et al., 1999). The three known isoforms of ACIN1 in humans, ACINUS-L, ACINUS-S and ACINUS-S' (202, 98, and 94 KDa, respectively) share similar three-dimensional structures, such as an RNA recognition motif and a C-terminal arginine–serine (RS) rich domain (Deka and Singh, 2019; Rodor et al., 2016; Vucetic et al., 2008). Deka and Singh (2019) reported that the RS domain is involved in alternative splicing regulation in *HeLa* cells. ACIN1 human isoforms interacts with RNA-binding proteins, such as RNA Binding Protein With Serine Rich Domain 1 (RNPS1) and the Sin3A Associated Protein 18 (SAP18), which is found to be associated with the histone deacetylase protein Sin3-HDAC. The complex formed by these proteins is referred to as a component of the apoptosis and splicing-associated protein (ASAP) (Deka and Singh, 2019; Schwerk et al., 2003). During the splicing process, all the components of the ASAP complex play a crucial role in both constitutive and alternative splicing (Michelle et al., 2012). This complex has these functions conserved among eukaryotes, including in plants, where Chen et al. (2019) reported the existence of equivalence

* Corresponding author.
E-mail address: murilo.alves@ufc.br (M.S. Alves).

https://doi.org/10.1016/j.plgene.2024.100459
Received 22 July 2023; Received in revised form 8 June 2024; Accepted 10 June 2024
Available online 13 June 2024

Plant Gene 34 (2023) 100407

Contents lists available at ScienceDirect

Plant Gene

journal homepage: www.elsevier.com/locate/plantgene

Genome-wide comparative analysis of *Glycolate oxidase* (*GOX*) gene family in plants

Érica Monik Silva Roque, Felipe de Castro Teixeira, Alex Martins de Aguiar, Victor Breno Faustino Bezerra, Ana Carolina Moreira da Costa, Sâmia Alves Silva, Ana Luiza Sobral Paiva, Humberto Henrique de Carvalho, Murilo Siqueira Alves *

Departamento de Bioquímica e Biologia Molecular, Universidade Federal do Ceará, Avenida Humberto Monte S/N, Campus Pici, Fortaleza, CE 60440-900, Brasil

ARTICLE INFO

Edited by E.T. Johnson

Keywords:
Genome-wide comparative analysis
Photorespiration
Synteny analysis
Gene family evolution
Glycolate metabolism

ABSTRACT

Glycolate Oxidase (GOX) is a key enzyme in photorespiration, a complex metabolic pathway in plants that affects photosynthesis efficiency and one of its most prominent products is hydrogen peroxide (H_2O_2). Photosynthetic pathways and H_2O_2 production can drastically differ between C3 and C4 plants which have distinctions in the photorespiration machinery. Such contrasts critically impact physiological processes in plants, such as development and stress responses. However, few studies bring light to evolutionary and structural aspects of the photorespiration components, and comparative analyses of gene families related to photorespiration in C3 and C4 plants are lacking. In the present study, we present the first genome-wide comparative analysis of the *GOX* gene family in plants, comparing relevant evolutionary and structural aspects of distinct *GOX* orthologs in plant families. The evolutionary relationships, gene structure, conserved motifs, promoter *cis*-element prediction, chromosome location, and interspecific collinearity were analyzed in order to gain a better understanding of the *GOX* gene family in plants. Family-dependent evolutionary and structural divergence were observed among distinct *GOX* genes, with higher gene conservation among *Fabaceae* family members. High sequence divergence found among *Fabaceae* and *Poaceae GOX* orthologs may impact functional divergence among these gene families. This comparative study provides a comprehensive picture of evolutionary and structural aspects of the *GOX* gene family in plants, as well as emphasizes the involvement of *GOX* orthologs in plant stress responses.

1. Introduction

Photosynthesis is a key process to land plants success, but some species have diverged evolutionarily in how to perform it. Most plants are divided by C3 and C4 nomenclature, which differ in biochemical and anatomical traits and subtraits to perform each type of photosynthesis (Gowik and Westhoff, 2011). The so-called C3 plants have their photosynthetic pathway (glycolate pathway) occurring commonly in all mesophyll cells. The CO_2 is carboxylated by RuBisCO, being converted into two molecules of 3-phosphoglycerate (3PG), which are then led to the Calvin-Benson Cycle. However, photorespiration in C3 plants starts in the chloroplasts with the oxygenase activity of RuBisCO, producing phosphoglycolate (2-PG), which will be converted into glycolate by 2-PG phosphatase (PGP). The glycolate is transferred to peroxisomes, where it will be oxidized to glyoxylate by the enzyme glycolate oxidase (GOX), resulting in hydrogen peroxide (H_2O_2) release (Foyer et al., 2009) (Fig. 1).

On the other hand, the C4 plant photosynthesis acts as a CO_2 "pump" and inhibits the oxygenation of RuBisCO by increasing the intracellular CO_2/O_2 ratio, normally using two types of cells: mesophyll and bundle sheath cells (Von Caemmerer and Furbank, 2003; Eisenhut et al., 2019). In the Hatch-Slack pathway (C4 photosynthesis), the dioxide (CO_2) molecule accumulation occurs in the vicinity of RuBisCO, impairing molecular oxygen (O_2) to reach the active site of RuBisCO. The carbon fixation process in C4 plants occurs in the mesophyll cells, where it is fixed in 4-carbon compounds such as oxaloacetate (OAA) by PEP carboxylase. The OAA is converted into malic acid (MAL) by NADP-malate dehydrogenase, or aspartic acid (ASP) by aspartate aminotransferase. Then, the MAL or ASP are decarboxylated in bundle sheath cells and fixed into 3-carbon compounds by the Calvin Cycle (Furbank, 2011; Langdale, 2011). Some plant species are C3-C4 intermediates. These species have bundle sheath characteristics similar to C4 plants and

* Corresponding author.
E-mail address: murilo.alves@ufc.br (M.S. Alves).

https://doi.org/10.1016/j.plgene.2023.100407
Received 21 August 2022; Received in revised form 28 January 2023; Accepted 1 February 2023
Available online 4 February 2023

plant biology

Plant Biology ISSN 1435-8603

RESEARCH ARTICLE

Genome-wide identification and characterization of SNW/SKIP domain-containing proteins in plants

S. A. Silva, V. B. F. Bezerra, F. C. Teixeira, E. M. S. Roque, J. I. B. do Nascimento, A. M. Aguiar, H. H. de Carvalho & M. S. Alves

Departamento de Bioquímica e Biologia Molecular, Universidade Federal do Ceará, Fortaleza, Brazil

Keywords
Gene family evolution; genome-wide comparative analysis; protein interaction network; protein physicochemical parameters; stress tolerance.

Correspondence
M. S. Alves, Departamento de Bioquímica e Biologia Molecular, Universidade Federal do Ceará, Avenida Humberto Monte S/N, Campus do Pici, Fortaleza, CE 60440-900, Brazil.
E-mail: murilo.alves@ufc.br

Editor
X.-Q. Wang

Received: 20 February 2024;
Accepted: 7 May 2024

doi:10.1111/plb.13676

ABSTRACT

- Sessile organisms, such as plants, developed various ways to sense and respond to external and internal stimuli to maximize their fitness through evolutionary time. Transcripts and protein regulation are, among many, the main mechanisms that plants use to respond to environmental changes. SKIP protein is one such, presenting an SNKW interacting domain, which is highly conserved among eukaryotes, where SKI interacting protein acts in regulating key processes.
- In the present work, many bioinformatics tools, such as phylogenetic relationships, gene structure, physical–chemical properties, conserved motifs, prediction of regulatory *cis*-elements, chromosomal localization, and protein–protein interaction network, were used to better understand the genome-wide SNW/SKIP domain-containing proteins.
- In total, 28 proteins containing the SNW/SKIP domain were identified in different plant species, including plants of agronomic interest. Two main protein clusters were formed in phylogenetic analysis, and gene structure analysis revealed that, in general, the coding region had no introns. Also, expression of these genes is possibly induced by abiotic stress stimuli. Primary structure analysis of the proteins revealed the existence of an evolutionarily conserved functional unit. But physicochemical properties show that proteins containing the SNW/SKIP domain are commonly unstable under *in vivo* conditions.
- In addition, the protein network, demonstrated that SKIP homologues could act by modulating plant fitness through gene expression regulation at the transcriptional and post-transcriptional levels. This could be corroborated by the expression number of gene copies of SKIP proteins in many species, highlighting it's crucial role in plant development and tolerance through the course of evolution.

INTRODUCTION

Plants have played a dynamic role in formation of the human race. About 12,000 years ago, during the Neolithic period, acquisition of knowledge and technology allowed the development of agriculture. This event completely changed the diet, lifestyle, and structure of human societies (Murphy 2007). Thus, plants were essential in establishment of the first civilizations and have ensured the evolution of mankind by providing a constant source of foods, beverages, fuels, and medicines. But because of their sessile nature, these important organisms must respond to the external environment and internal signals to regulate their development and environmental fitness (Cao & Ma 2019; Ghazaryab *et al.* 2023; Singh *et al.* 2023a). To respond accurately to these signals in eukaryotes, gene expression is controlled at several levels, mostly at the transcriptional and post-transcriptional levels (Licatalosi & Darnell 2010; Cao & Ma 2019). This allows a gene to be expressed at the correct location and time, as well as in the appropriate abundance to sustain its function, through control of several proteins that participate in gene regulation (Cao & Ma 2019). Among these proteins, the SKI interacting protein (SKIP) is an evolutionarily conserved protein among eukaryotes (Folk *et al.* 2004).

The SKIP protein was first identified as a protein that interacts with cellular and viral forms of SKI, using the yeast double hybrid system (Dahl *et al.* 1998). SKI, in turn, is an oncoprotein that is involved in the induction of cell transformation (growth) and differentiation (Prathapam *et al.* 2001). Like SKI, SKIP is expressed in various tissue types and is localized to the cell nucleus (Dahl *et al.* 1998). The SKI-SKIP interaction was shown to be potentially important for SKI function, as SKIP can interact with a highly conserved region of SKI that is required for its transformation activity, the N-terminal region (Dahl *et al.* 1998; Prathapam *et al.* 2001). The SNW domain, which includes the signature peptide SNWKN, was identified as the region of the SKIP protein responsible for interacting with the SKI oncoprotein (Prathapam *et al.* 2001). The primary structure of SKIP is subdivided into the N- and C-terminal regions, separated by the central SNW domain. The C-terminal region is important for the localization and stability of the protein in cells, while the N-terminal region and the SNW domain